Ortho-CH Activation of Aromatic Ketones, Partially Fluorinated Aromatic Ketones, and Aromatic Imines by a Trihydride-Stannyl-Osmium(IV) Complex

Miguel A. Esteruelas,*[,†] Agustí Lledós,*[,‡] Montserrat Oliván,[†] Enrique Oñate,[†] María A. Tajada,[†] and Gregori Ujaque[‡]

Departamento de Química Inorgánica, Instituto de Ciencia de Materiales de Aragón, Universidad de Zaragoza-CSIC, 50009 Zaragoza, Spain, and Departament de Química, Edifici Cn, Universitat Autònoma de Barcelona, 08193 Bellaterra, Barcelona, Spain

Received March 27, 2003

Complex $OsH_3(SnPh_2Cl)\{\eta^2\text{-}CH_2{=}C(CH_3)P^iPr_2\}(P^iPr_3)$ (**1**) reacts with acetophenone and benzophenone to give $OsH_2(SnPh_2Cl)\{C_6H_4C(O)R\}(P^iPr_3)_2$ (R = CH_3 (**2**), Ph (**3**)). In the solid state, the structure of **2** determined by X-ray diffraction analysis can be described as a pentagonal bipyramid with the phosphorus atoms of the phosphines occupying axial positions. In solution the hydride ligands of **2** and **3** undergo a thermally activated site exchange process. The activation parameters for the exchange are $\Delta H^{\ddagger} = 11.9 \pm 0.5$ kcal·mol^{-1} and $\Delta S^{\ddagger} = -0.7 \pm 1.2$ cal·mol^{-1}·K^{-1} for **2** and $\Delta H^{\ddagger} = 11.8 \pm 0.2$ kcal·mol^{-1} and $\Delta S^{\ddagger} = -2.6 \pm 1.9$ cal·mol^{-1}·K^{-1} for **3**. The reaction of **1** with perdeuterated benzophenone affords the hydride-deuteride $Os(H)(D)(SnPh_2Cl)\{C_6D_4C(O)C_6D_5\}(P^iPr_3)_2$ (**3-*d*$_{10}$**), suggesting that the activation takes place on the monohydride intermediate $OsH(SnPh_2Cl)(P^iPr_3)_2$. The reaction pathway for the formation of this intermediate is evaluated by DFT calculations. Complex **1** also reacts with 2,3,4,5,6-pentafluorobenzophenone, 2-fluoroacetophenone, and benzophenone imine. The reactions with the partially fluorinated ketones give $OsH_2(SnPh_2Cl)\{C_6H_4C(O)C_6F_5\}(P^iPr_3)_2$ (**4**) and $OsH_2(SnPh_2Cl)\{C_6H_3FC(O)CH_3\}(P^iPr_3)_2$ (**5**). In solution, the hydride ligands of **4** and **5** also exchange their positions. In this case, the activation parameters are $\Delta H^{\ddagger} = 12.6 \pm 0.5$ kcal·mol^{-1} and $\Delta S^{\ddagger} = -2.9 \pm 1$ cal·mol^{-1}·K^{-1} for **4** and $\Delta H^{\ddagger} = 11.2 \pm 0.4$ kcal·mol^{-1} and $\Delta S^{\ddagger} = -2.8 \pm 1.1$ cal·mol^{-1}·K^{-1} for **5**. The reaction of **1** with benzophenone imine leads to $OsH_2(SnPh_2Cl)\{C_6H_4C(NH)C_6H_5\}(P^iPr_3)_2$ (**6**), which has been characterized by X-ray diffraction analysis. The structure reveals an intramolecular Cl···H−N hydrogen bond between the chlorine bonded to the tin atom and the hydrogen of the imine. Treatment of **6** with KOH affords $OsH_2(SnPh_2OH)\{C_6H_4C(NH)C_6H_5\}(P^iPr_3)_2$ (**7**). The X-ray diffraction analysis of **7** shows a intramolecular O···H−N hydrogen bond and intermolecular HO···H interactions between the oxygen and the O−H hydrogen atom of two adjacent molecules in the crystal. DFT calculations on the model compounds $OsH_2\{Sn(CH{=}CH_2)_2Cl\}\{C_6H_4C(O)CH_3\}(PH_3)_2$ (**2t**) and $OsH_2\{Sn(CH{=}CH_2)_2X\}\{C_6H_4C(NH)CH_3\}(PH_3)_2$ (X = Cl (**6t**), OH (**7t**)) have allowed the complete determination of the hydride positions in **2**, **6**, and **7** and the full characterization of the hydrogen bonds in **6** and **7**.

Introduction

The activation of C−H bonds by transition metal compounds is a type of reaction of general interest due to its connection with the functionalization of nonactivated organic molecules.[1] An example is the Murai reaction.

In 1993, Murai and co-workers reported that the C−H bond at the *ortho* position of aromatic ketones selectively adds to the double bond of olefins using the ruthenium complex $RuH_2(CO)(PPh_3)_3$ as catalyst.[2]

Murai's reaction is now one of the most important processes in organic synthesis, which allows the alkylation of aromatic ketones,[3] esters,[4] and imines,[5] as well

[†] Universidad de Zaragoza
[‡] Universitat Autònoma de Barcelona

(1) (a) Shilov, A. E.; Shul'pin, G. B. *Chem. Rev.* **1997**, *97*, 2879. (b) Jia, C.; Kitamura, T.; Fujiwara, Y. *Acc. Chem. Res.* **2001**, *34*, 633. (c) Ritleng, V.; Sirlin, C.; Pfeffer, M. *Chem. Rev.* **2002**, *102*, 1731.

(2) Murai, S.; Kakiuchi, F.; Sekine, S.; Tanaka, Y.; Kamatani, A.; Sonoda, M.; Chatani, N. *Nature* **1993**, *366*, 529.

(3) (a) Kakiuchi, F.; Sekine, S.; Tanaka, Y.; Kamatani, A.; Sonoda, M.; Chatani, N.; Murai, S. *Bull. Chem. Soc. Jpn.* **1995**, *68*, 62. (b) Murai, S.; Chatani, N.; Kakiuchi, F. *Pure Appl. Chem.* **1997**, *69*, 589.

(4) Sonoda, M.; Kakiuchi, F.; Kamatani, A.; Chatani, N.; Murai, S. *Chem. Lett.* **1996**, 109.

(5) Kakiuchi, F.; Yamauchi, M.; Chatani, N.; Murai, S. *Chem. Lett.* **1996**, 111.

10.1021/om030229y CCC: $25.00
Publication on Web 08/08/2003

as the copolymerization of aromatic ketones and α,ω-divinylsilanes.[6] Experimental evidence and theoretical calculations suggest that the above-mentioned reactions involve the selective *ortho*-CH activation of the aromatic ring of the substrate by the d^8 intermediate Ru(CO)-$(PPh_3)_3$, which is formed by hydrogen transfer from the dihydride $RuH_2(CO)(PPh_3)_3$ to the olefin.[7] Sabo-Etienne and Chaudret have observed that the dihydride-bisdihydrogen derivative $RuH_2(\eta^2\text{-}H_2)_2(PCy_3)_2$ can also act as a catalyst precursor.[8]

Although the C−H activation with high-valent metal complexes is rare, we have observed that the saturated d^2 hexahydride $OsH_6(P^iPr_3)_2$ can be thermally activated. The resulting metallic fragment is capable of producing the triple C−H bond activation of the cyclohexyl group of cyclohexylmethyl ketone[9] and of activating *ortho*-CH and *ortho*-CF bonds in aromatic ketones. The *ortho*-CH activation is preferred over the *ortho*-CF activation in ketones containing only one aromatic ring. However, the *ortho*-CF activation is preferred over the *ortho*-CH activation in 2,3,4,5,6-pentafluorobenzophenone.[10]

The use of transition metal tin compounds in the catalysis of organic transformations is attracting a great deal of attention. Tin ligands have a strong labilizing effect on their *trans* ligands and are also quite labile themselves; thus, they promote migratory insertions or provide vacant coordination sites on the transition metal by dissociation. Furthermore, hydride-stannyl derivatives undergo easy oxidative addition and subsequent reductive elimination.[11]

In an effort to introduce the advantages of the tin ligands in the osmium-polyhydrides, we have recently prepared the trihydride-stannyl compound $OsH_3(SnPh_2Cl)\{\eta^2\text{-}CH_2{=}C(CH_3)P^iPr_2\}(P^iPr_3)$.[12] In this paper, we report the reactions of this complex with aromatic ketones, partially fluorinated aromatic ketones, and benzophenone imine.

Results and Discussion

1. Reactions with Aromatic Ketones. Treatment at room temperature of toluene solutions of $OsH_3(SnPh_2Cl)\{\eta^2\text{-}CH_2{=}C(CH_3)P^iPr_2\}(P^iPr_3)$ (**1**) with 1.5 equiv of acetophenone and benzophenone affords orange-red solutions, from which the dihydride-stannyl derivatives $OsH_2(SnPh_2Cl)\{C_6H_4C(O)R\}(P^iPr_3)_2$ (R = CH_3 (**2**), Ph (**3**)) were isolated as orange (**2**) or red (**3**) solids in high yield (71% (**2**), 62% (**3**)). These complexes are the result of the reduction of the isopropenyl group of the isopropenylphosphine of **1** and the C−H activation of one of the *ortho*-CH bonds of the ketones (eq 1).

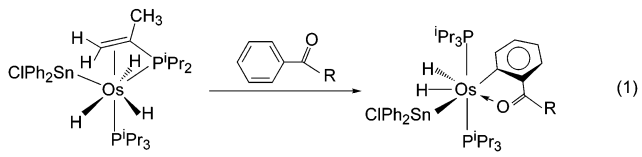

1 R = CH_3 (**2**), Ph (**3**) (1)

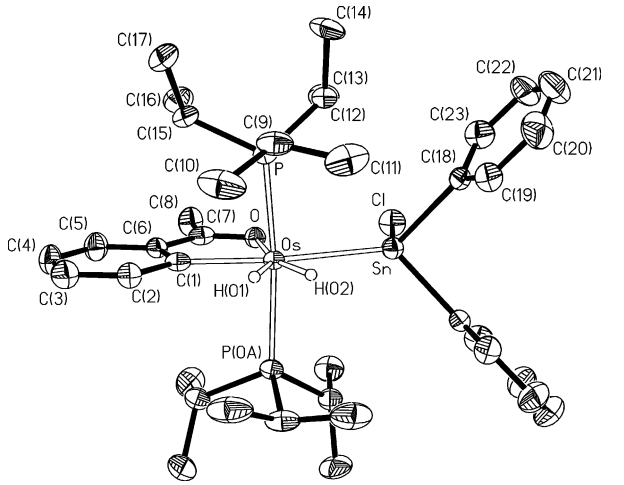

Figure 1. Molecular diagram of the complex $OsH_2(SnPh_2Cl)\{C_6H_4C(O)CH_3\}(P^iPr_3)_2$ (**2**).

Table 1. Selected Bond Distances (Å) and Angles (deg) for the Complex $OsH_2(SnPh_2Cl)\{C_6H_4C(O)CH_3\}(P^iPr_3)_2$ (2)

Os−Sn	2.7169(4)	Sn−Cl	2.4331(14)
Os−P	2.3930(9)	O−C(7)	1.269(6)
Os−O	2.145(3)	C(1)−C(6)	1.407(7)
Os−C(1)	2.068(5)	C(6)−C(7)	1.418(7)
Os−H(01)	1.40(4)	C(7)−C(8)	1.495(6)
Os−H(02)	1.49(4)		

Sn−Os−P	94.60(2)	O−Os−H(02)	160.8(16)
Sn−Os−O	85.22(9)	C(1)−Os−H(01)	75.2(17)
Sn−Os−C(1)	161.61(14)	C(1)−Os−H(02)	122.8(16)
Sn−Os−H(01)	123.2(17)	H(01)−Os−H(02)	47.6(19)
Sn−Os−H(02)	75.6(16)	Os−Sn−Cl	110.36(4)
C(18)−Sn−Cl	96.67(10)	Os−Sn−C(18)	126.08(9)
C(18)−Sn−C(018)	94.12(18)	P−Os−P(0A)	165.47(5)
Os−O−C(7)	115.9(3)	P−Os−O	95.98(2)
Os−C(1)−C(6)	115.0(4)	P−Os−C(1)	87.41(3)
C(1)−C(6)−C(7)	114.6(5)	P−Os−H(01)	82.78(4)
O−C(7)−C(6)	118.1(5)	P−Os−H(02)	85.71(17)
O−C(7)−C(8)	117.1(5)	O−Os−C(1)	76.39(16)
C(6)−C(7)−C(8)	124.8(5)	O−Os−H(01)	151.6(17)

A view of the molecular geometry of **2** is shown in Figure 1. Selected bond distances and angles are listed in Table 1. The coordination geometry around the osmium atom can be rationalized as a distorted pentagonal bipyramid with the two phosphorus atoms of the triisopropylphosphine ligands occupying axial positions (P−Os−P = 165.47(5)°). The osmium sphere is completed by the orthometalated ketone, which acts with a bite angle of 76.39(16)°, the stannyl ligand *cisoid* disposed to the oxygen atom of the ketone (O−Os−Sn = 85.22 (9)°) and the hydride ligands.

(6) (a) Guo, H.; Weber, W. P. *Polym. Bull.* **1994**, *32*, 525. (b) Tapsak, M. A.; Guo, H.; Weber, W. P. *Polym. Bull.* **1995**, *34*, 49. (c) Guo, H.; Wang, G.; Tapsak, M. A.; Weber, W. P. *Macromolecules* **1995**, *28*, 5686.

(7) (a) Colombo, M.; George, M. W.; Moore, J. N.; Pattison, D. I.; Perutz, R. N.; Virrels, I. G.; Ye, T.-Q. *J. Chem. Soc., Dalton Trans.* **1997**, 2857. (b) Matsubara, T.; Koga, N.; Musaev, D. G.; Morokuma, K. *J. Am. Chem. Soc.* **1998**, *120*, 12692. (c) Matsubara, T.; Koga, N.; Musaev, D. G.; Morokuma, K. *Organometallics* **2000**, *19*, 2318.

(8) Guari, Y.; Sabo-Etienne, S.; Chaudret, B. *J. Am. Chem. Soc.* **1998**, *120*, 4228.

(9) Barrio, P.; Castarlenas, R.; Esteruelas, M. A.; Oñate, E. *Organometallics* **2001**, *20*, 2635.

(10) Barrio, P.; Castarlenas, R.; Esteruelas, M. A.; Lledós, A.; Maseras, F.; Oñate, E.; Tomàs, J. *Organometallics* **2001**, *20*, 442.

(11) Holt, M. S.; Wilson, W. L.; Nelson, J. H. *Chem. Rev.* **1989**, *89*, 11.

(12) (a) Tajada, M. A. Ph.D. Dissertation, University of Zaragoza, 2003. (b) Esteruelas, M. A.; Lledós, A.; Maseras, F.; Oliván, M.; Oñate, E.; Tajada, M. A.; Tomàs, J. *Organometallics* **2003**, *22*, 2087.

The Os−C(1) bond length of 2.068(5) Å is typical for an Os−C(aryl) single bond and agrees well with the values previously found in other orthometalated osmium compounds (between 2.06 and 2.14 Å).[10,13] The Os−O distance of 2.145(3) Å is that expected for a single bond, whereas the O−C(7) bond length (1.269(6) Å) is similar to that found in free acetophenone (1.217 Å).[14]

The Os−Sn distance (2.7169(4) Å) agrees well with those reported for other mononuclear osmium-stannyl derivatives (2.6−2.7 Å),[15] while it is about 0.1 Å shorter than the Os(μ-H)Sn−osmium−tin bond length in the cluster $[Os_3SnH_2(CO)_{10}\{CH(SiMe_3)_2\}_2]$ (2.855(3) Å).[16] The environment of the tin atom is tetrahedral, with the chlorine atom lying in the equatorial plane of the bipyramid. The angles around the tin atom are between 94.12(18)° (C−Sn−C) and 126.08(9)° (C−Sn−Os).

The hydride positions obtained from X-ray diffraction data are, in general, imprecise.[17] However, DFT calculations have been shown to provide useful accurate data for the hydrogen positions in both classical polyhydride[18] and dihydrogen[19] complexes. So, to corroborate the structure of **2**, a DFT study on the model complex $OsH_2\{Sn(CH{=}CH_2)_2Cl\}\{C_6H_4C(O)CH_3\}(PH_3)_2$ (**2t**) has been carried out. Figure 2 shows its B3LYP optimized structure, whereas its main geometrical parameters are collected in Table 2. Bond distances and angles for the non-hydrogen atoms of **2t** agree well with those determined by X-ray diffraction for **2**.

As expected, the Os−H distances are about 1.6 Å (Os−H(1) = 1.632 Å and Os−H(2) = 1.664 Å), while the separation between the hydride ligands is 1.712 Å. This clearly supports the dihydride character of **2**. There is no interaction between the tin atom and the hydride ligand H(2). The separation between them (2.403 Å) is between 0.8 and 0.6 Å longer than the bond length in tin-hydride compounds of the type H−SnR_3.[20]

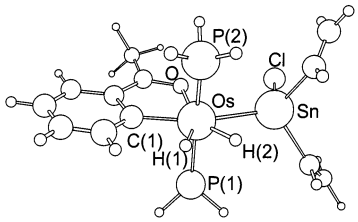

Figure 2. B3LYP optimized structure of the model complex $OsH_2\{Sn(CH{=}CH_2)_2Cl\}\{C_6H_4C(O)CH_3\}(PH_3)_2$ (**2t**).

Table 2. Optimized (B3LYP) Distances (Å) and Angles (deg) of $OsH_2\{Sn(CH{=}CH_2)_2Cl\}\{C_6H_4C(O)CH_3\}(PH_3)_2$ (2t)

Os−Sn	2.739	Os−P(1)	2.333
Os−P(2)	2.333	Os−O	2.188
Os−C(1)	2.120	Os−H(1)	1.632
Os−H(2)	1.664	Sn−Cl	2.472
H(1)···H(2)	1.712	Sn···H(2)	2.403
P(1)−Os−P(2)	174.914	Sn−Os−P(1)	90.736
Sn−Os−P(2)	91.612	Sn−Os−O	82.375
Sn−Os−C(1)	157.941	O−Os−P(1)	92.502
C(1)−Os−P(1)	89.579	O−Os−P(2)	92.284
C(1)−Os−P(2)	89.937	O−Os−C(1)	75.577
H(1)−Os−Sn	123.035	H(2)−Os−Sn	60.462
H(1)−Os−P(1)	87.421	H(2)−Os−P(1)	88.717
H(1)−Os−P(2)	87.510	H(2)−Os−P(2)	88.512
H(1)−Os−C(1)	79.014	H(2)−Os−C(1)	141.589
H(1)−Os−O	154.589	H(2)−Os−O	142.834
H(1)−Os−H(2)	62.576		

In agreement with the presence of the hydride and metalated ketone ligands, the IR spectra of **2** and **3** contain ν(Os−H) and ν(C═O) bands at 2086 (**2**) and 2114 (**3**) cm^{-1} and 1590 (**2**) and 1666 (**3**) cm^{-1}, respectively.

The ^1H NMR spectra are temperature-dependent. At 303 K in toluene as solvent, the spectrum of **2** shows in the hydride region a broad resonance centered at −11.86 ppm. At about 273 K decoalescence occurs, and at 233 K, an ABX_2 spin system defined by $\delta_A = -11.02$, $\delta_B = -13.01$, $J_{A-X} = J_{B-X} = 14$ Hz, and $J_{A-B} = 46$ Hz is observed. The variation of the hydride resonance of **3** is like that of **2**. At 303 K, the spectrum contains a broad hydride resonance centered at −11.40 ppm. At about 273 K decoalescence occurs, and at 233 K, an ABX_2 spin system defined by $\delta_A = -10.45$, $\delta_B = -12.54$, $J_{A-X} = 9$ Hz, $J_{B-X} = 12.6$ Hz, and $J_{A-B} = 42$ Hz is observed.

The dependence on the temperature of these spectra indicates that the hydride ligands undergo a thermally activated site exchange process. Line-shape analysis of the $^1H\{^{31}P\}$ NMR spectra (Figure 3 shows those of **2**) allows the calculation of the rate constants for the process at each temperature (Table 3). The activation parameters obtained from the corresponding Eyring analysis are $\Delta H^{\ddagger} = 11.9 \pm 0.5$ kcal·mol^{-1} and $\Delta S^{\ddagger} = -0.7 \pm 1.2$ cal·mol^{-1}·K^{-1} for **2** and $\Delta H^{\ddagger} = 11.8 \pm 0.2$

(13) (a) Esteruelas, M. A.; Lahoz, F. J.; López, A. M.; Oñate, E.; Oro, L. A. *Organometallics* **1995**, *14*, 2496. (b) Esteruelas, M. A.; Lahoz, F. J.; Oñate, E.; Oro, L. A.; Sola, E. *J. Am. Chem. Soc.* **1996**, *118*, 89. (c) Buil, M. L.; Esteruelas, M. A.; López, A. M.; Oñate, E. *Organometallics* **1997**, *16*, 3169. (d) Crochet, P.; Esteruelas, M. A.; Gutiérrez-Puebla, E. *Organometallics* **1998**, *17*, 3141. (e) Esteruelas, M. A.; Gutiérrez-Puebla, E.; López, A. M.; Oñate, E.; Tolosa, J. I. *Organometallics* **2000**, *19*, 275. (f) Baya, M.; Crochet, P.; Esteruelas, M. A.; Oñate, E.; *Organometallics* **2001**, *20*, 240. (g) Baya, M.; Esteruelas, M. A.; Oñate, E. *Organometallics* **2001**, *20*, 4875.

(14) 3D Search and Research Using the Cambridge Structural Data Base: Allen, F. H.; Kennard, O. *Chem. Des. Autom. News* **1993**, *8*, 31.

(15) (a) Clark, A. M.; Rickard, C. E. F.; Roper, W. R.; Wright, L. J. *J. Organomet. Chem.* **1997**, *543*, 111. (b) Clark, A. M.; Rickard, C. E. F.; Roper, W. R.; Woodman, T. J.; Wright, L. J. *Organometallics* **2000**, *19*, 1766.

(16) Cardin, C. J.; Cardin, D. J.; Parge, H. E.; Power, J. M. *J. Chem. Soc., Chem. Commun.* **1984**, 609.

(17) Zhao, D.; Bau, R. *Inorg. Chim. Acta* **1998**, *269*, 162.

(18) See for example: (a) Lin, Z.; Hall, M. B. *Inorg. Chem.* **1991**, *30*, 2569. (b) Lin, Z.; Hall, M. B. *Coord. Chem. Rev.* **1994**, *135*, 845. (c) Esteruelas, M. A.; Jean, Y.; Lledós, A.; Oro, L. A.; Ruiz, N.; Volatron, F. *Inorg. Chem.* **1994**, *33*, 3609. (d) Camanyes, S.; Maseras, F.; Moreno, M.; Lledós, A.; Lluch, J. M.; Bertrán, J. *J. Am. Chem. Soc.* **1996**, *118*, 4617. (e) Demachy, I.; Esteruelas, M. A.; Jean, Y.; Lledós, A.; Maseras, F.; Oro. L. A.; Valero, C.; Volatron, F. *J. Am. Chem. Soc.* **1996**, *118*, 8388. (f) Castillo, A.; Barea, G.; Esteruelas, M. A.; Lahoz, F. J.; Lledós, A.; Maseras, F.; Modrego, J.; Oñate, E.; Oro, L. A.; Ruiz, N.; Sola, E. *Inorg. Chem.* **1999**, *38*, 1814. (g) Buil, M. L.; Esteruelas, M. A.; Modrego, J.; Oñate, E. *New J. Chem.* **1999**, *23*, 403. (h) Castarlenas, R.; Esteruelas, M. A.; Gutiérrez-Puebla, E.; Jean, Y.; Lledós, A.; Martín, M.; Tomàs, J. *Organometallics* **1999**, *18*, 4296. (i) Maseras, F.; Lledós, A.; Clot, E.; Eisenstein, O. *Chem. Rev.* **2000**, *100*, 601.

(19) See for example: (a) Dapprich, S.; Frenking, G. *Angew. Chem., Int. Ed. Engl.* **1995**, *34*, 354. (b) Bakhmutov, V. I.; Bertrán, J.; Esteruelas, M. A.; Lledós, A.; Maseras, F.; Modrego, J.; Oro, L. A.; Sola, E. *Chem. Eur. J.* **1996**, *2*, 815. (c) Maseras, F.; Lledós, A.; Costa, M.; Poblet, J. M. *Organometallics* **1996**, *15*, 2947. (d) Gelabert, R.; Moreno, M.; Lluch, J. M.; Lledós, A. *Organometallics* **1997**, *16*, 3805. (e) Albéniz, M. J.; Esteruelas, M. A.; Lledós, A.; Maseras, F.; Oñate, E.; Oro, L. A.; Sola, E.; Zeier, B. *J. Chem. Soc., Dalton Trans.* **1997**, 181. (f) Barea, G.; Esteruelas, M. A.; Lledós, A.; López, A. M.; Oñate, E.; Tolosa, J. I. *Organometallics* **1998**, *17*, 4065. (g) Barea, G.; Esteruelas, M. A.; Lledós, A.; López, A. M.; Tolosa, J. I. *Inorg. Chem.* **1998**, *37*, 5033.

(20) (a) Schager, F.; Goddard, R.; Seevogel, K.; Pörschke, K.-R. *Organometallics* **1998**, *17*, 1546. (b) Schumann, H.; Wassermann, B. C.; Frackowiak, M.; Omotowa, B.; Schutte, S.; Velder, J.; Mühle, S. H.; Krause, W. *J. Organomet. Chem.* **2000**, *609*, 189. (c) Sasaki, K.; Kondo, Y.; Maruoka, K. *Angew. Chem., Int. Ed.* **2001**, *40*, 411.

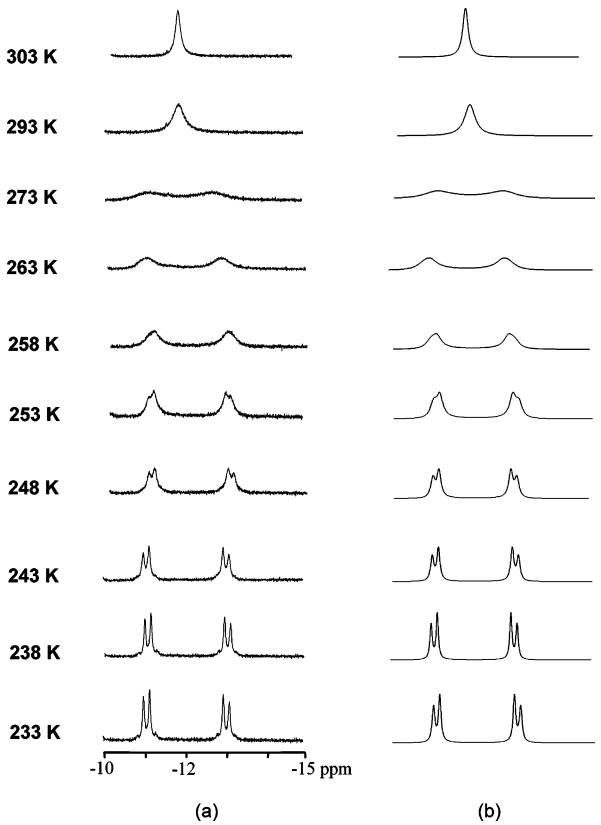

Figure 3. (a) Variable-temperature $^1H\{^{31}P\}$ NMR spectra (300 MHz) in C_7D_8 in the high-field region of $OsH_2(SnPh_2Cl)\{C_6H_4C(O)CH_3\}(P^iPr_3)_2$ (**2**). (b) Simulated spectra.

Table 3. Rate Constants for the Hydride Exchange of Complexes 2, 3, 4, and 5

	rate (s^{-1})			
T (K)	**2**	**3**	**4**	**5**
333		3.23×10^4		6.97×10^3
313		8.82×10^3	2.50×10^4	1.96×10^3
303	1.18×10^4			
293	6.13×10^3	2.13×10^3	6.84×10^3	4.65×10^2
283			2.95×10^3	
273	7.08×10^2	4.37×10^2	1.22×10^3	1.40×10^2
263	3.72×10^2		6.57×10^2	
258	2.45×10^2			
253	1.59×10^2	50	2.57×10^2	10
248	1.01×10^2			
243	68.8		1.10×10^2	
238	42			
233	53.1	21.9		

kcal·mol^{-1} and $\Delta S^{\ddagger} = -2.6 \pm 1.9$ cal·mol^{-1}·K^{-1} for **3**. The values for the entropy of activation close to zero are in agreement with an intramolecular process, while the values for the enthalpy of activation lie in the range reported for thermal exchange processes in trihydride, hydride-dihydrogen, and dihydride derivatives.[18f,h,21]

To estimate the hydrogen−hydrogen separation between the hydride ligands of **2** and **3** in solution, the T_1 values of the hydride resonances were also determined over the temperature range 273−223 K. The same $T_{1(min)}$ values were found for both compounds and for each resonance (81 ± 4 ms). It occurs at 238 K for **2** and 243 K for **3**. The total relaxation rate for H_n ($R_n = 1/T_{1(min)}(H_n)$) is the addition of the relaxation rate due to the dipole−dipole interaction (R_{H-H}) and that due to all other relaxation contributors (R^*). Since the latter has been estimated as 2.5 s^{-1},[22] we can determine that the relaxation rate due to the hydride−hydride interaction is 9.8 s^{-1}. Using the standard equation,[23] this value leads to a separation between the hydride ligands of **2** and **3** of 1.54 Å, which is about 0.16 Å shorter than that obtained by theoretical methods.

The $^{31}P\{^1H\}$ NMR spectra are also temperature-dependent. At 293 K, the spectrum of **2** shows a singlet at 7.4 ppm, along with the tin satellites ($J_{P-^{119}Sn} = J_{P-^{117}Sn} = 113$ Hz). Lowering the sample temperature leads to broadening of the resonance. At 203 decoalescence occurs, and at 183 K, an AB spin system centered at 6.9 ppm, and defined by $\Delta\nu = 549$ Hz and $J_{A-B} = 202$ Hz, is observed. The behavior of the resonance of **3** with the temperature is the same as that of **2**. At 293 K, the spectrum contains a singlet at 7.9 ppm, along with the tin satellites ($J_{P-^{119}Sn} = J_{P-^{117}Sn} = 119$ Hz), while at 193 K, an AB spin system centered at 7.7 ppm, and defined by $\Delta\nu = 578$ Hz and $J_{A-B} = 195$ Hz, is observed. The presence of AB spin systems in the spectra at low temperature is consistent with the existence of a single conformer in which the *trans* phosphines are inequivalent due to hindered rotation about the Os−P or/and Os−Sn bonds. Resistance to rotation about these single bonds could be a consequence of the steric hindrance experienced by the isopropyl groups of the phosphines and the phenyl groups of the stannyl ligand. In this context, it should be noted the strong deviation of the C′−Sn−C angle from the ideal value of 109°. A similar behavior has been previously observed for some five- and six-coordinate ruthenium and osmium complexes containing bulky phosphine ligands.[24]

In the $^{13}C\{^1H\}$ NMR spectra, the most noticeable resonances are those due to the carbonyl and metalated carbon atoms of the ketone. In the $^{13}C\{^1H\}$ NMR spectrum of **2**, at room temperature, the carbonyl carbon atom displays a triplet at 212.7 ppm with a C−P coupling constant of 2 Hz, whereas the resonance due to the metalated carbon atom is observed as a triplet at 194.9 ppm, with a C−P coupling constant of 7 Hz. In the spectrum of **3**, the carbonyl resonance appears as a singlet at 208.5 ppm, and the metalated resonance is observed as a triplet at 198.1 ppm, with a C−P coupling constant of 7 Hz. At room temperature, the $^{119}Sn\{^1H\}$ NMR spectra show triplets at 15.2 (**2**) and 18.2 (**3**) ppm.

2. Mechanism of the Activation. On the basis of a low energy for the dissociation of molecular hydrogen

(21) See for example: (a) Earl, K. A.; Jia, G.; Maltby, P. A.; Morris, R. H. *J. Am. Chem. Soc.* **1991**, *113*, 3027. (b) Jia, G.; Drouin, S. D.; Jessop, P. G.; Lough, A. J., Morris, R. H. *Organometallics* **1993**, *12*, 906. (c) Esteruelas, M. A.; Lahoz, F. J.; López, A. M.; Oñate, E.; Oro, L. A.; Ruiz, N.; Sola, E.; Tolosa, J. I. *Inorg. Chem.* **1996**, *35*, 7811.

(22) Castillo, A.; Esteruelas, M. A.; Oñate, E.; Ruiz, N. *J. Am. Chem. Soc.* **1997**, *119*, 9691.

(23) At 300 MHz, $R_{H-H} = 129.18/r^6$. See: (a) Hamilton, D. G.; Crabtree, R. H. *J. Am. Chem. Soc.* **1988**, *110*, 4126. (b) Bautista, M. T.; Earl, K. A.; Maltby, P. A.; Morris, R. H.; Schweitzer, C. T.; Sella, A. *J. Am. Chem. Soc.* **1988**, *110*, 7031. (c) Desrosiers, P. J.; Cai, L.; Lin, Z.; Richards, R.; Halpern, J. *J. Am. Chem. Soc.* **1991**, *113*, 4173. (d) Gusev, D. G.; Kuhlman, R.; Sini, G.; Eisenstein, O.; Caulton, K. G. *J. Am. Chem. Soc.* **1994**, *116*, 2685.

(24) See for example: (a) Poulton, J. T.; Folting, K.; Streib, W. E.; Caulton, K. G. *Inorg. Chem.* **1992**, *31*, 3190. (b) Poulton, J. T.; Sigalas, M. P.; Folting, K.; Streib, W. E.; Eisenstein, O.; Caulton, K. G. *Inorg. Chem.* **1994**, *33*, 1476. (c) Notheis, J. U.; Heyn, R. H.; Caulton, K. G. *Inorg. Chim. Acta* **1995**, *229*, 187.

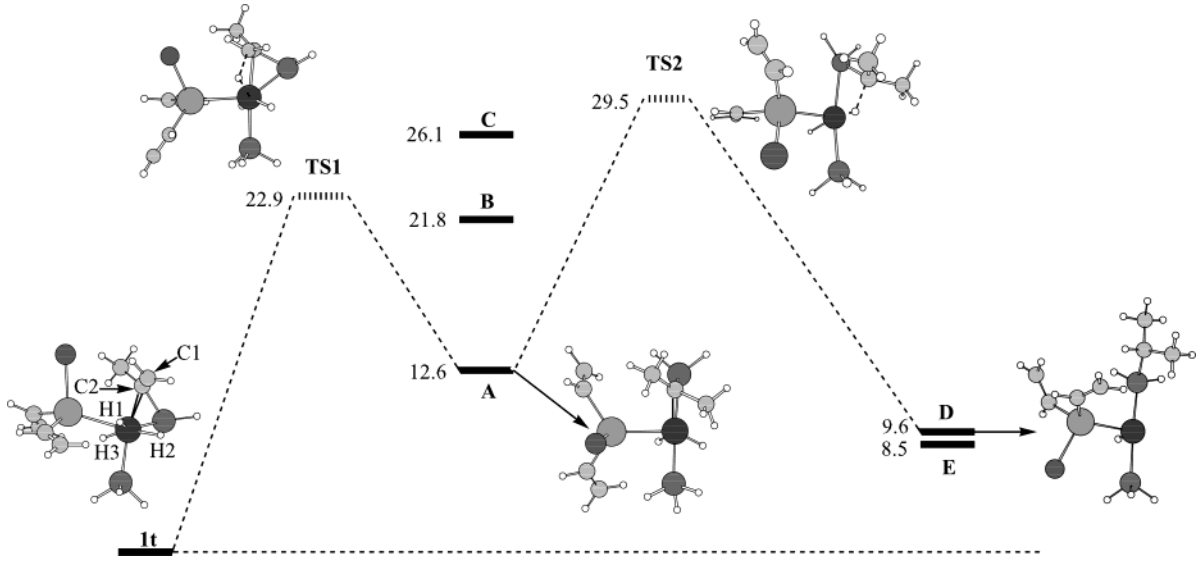

Figure 4. Energy profile (CCSD(T) level of theory) for the hydrogenation of the isopropenyl group of $OsH_3\{Sn(CH{=}CH_2)_2Cl\}\{\eta^2\text{-}CH_2{=}C(CH_3)PH_2\}(PH_3)$ (**1t**) (energies in kcal·mol^{-1}).

from $OsH_6(P^iPr_3)_2$,[25] it has been proposed that the *ortho*-CH activation of aromatic ketones with the hexahydride involves an unsaturated $OsH_2(\eta^2\text{-}H_2)(P^iPr_3)_2$ intermediate. The activation requires toluene under reflux conditions.[10]

In contrast to the reactions with $OsH_6(P^iPr_3)_2$, the activations shown in eq 1 occur at room temperature. At first glance, one could think that the difference in behavior between the hexahydride and **1** is related to the high lability of the isopropenyl group of the isopropenylphosphine of **1**. As a consequence of the constrained ring formed by the chelated isopropenylphosphine ligand and the osmium atom, complex **1** releases the coordinated carbon−carbon double bond.[12] Once the resulting unsaturated intermediate is formed, the *ortho*-CH activation of the corresponding ketone, followed by the hydrogenation of the isopropenyl group of the phosphine, should afford **2** and **3**. To corroborate this hypothesis, we carried out the reaction of **1** with perdeuterated benzophenone. Moreover, the reaction pathway leading to this activation has also been explored by means of theoretical calculations.

Treatment of **1** with perdeuterated benzophenone, under the same conditions as those previously mentioned for the formation of **3**, leads to a red solid in 52% yield. Interestingly, according to the ^2H and ^1H NMR spectra, the solid corresponds to the hydride-deuteride complex $Os(H)(D)(SnPh_2Cl)\{C_6D_4C(O)C_6D_5\}(P^iPr_3)_2$ (**3-d_{10}** in eq 2). Deuteration of the phosphine ligands is not observed.

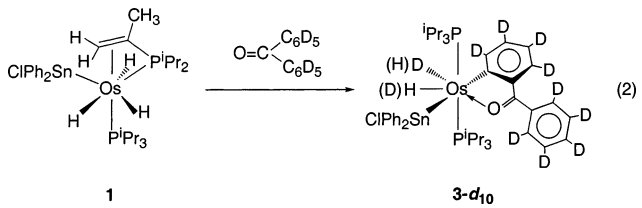

(2)

1 **3-d_{10}**

According to the presence of a deuterium atom at the metallic center, the ^2H NMR spectrum in toluene at 263 K shows, in addition to the phenyl resonances, two broad signals at −10.4 and −12.5 ppm in a 0.5:0.5 intensity ratio. In agreement with this spectrum, the ^1H NMR spectrum in toluene-d_8 at 233 K contains in the hydride region two triplets at −10.45 (J_{H-P} = 9 Hz) and −12.60 (J_{H-P} = 12.6 Hz) ppm, in a 0.5:0.5 intensity ratio.

The formation of **3-d_{10}** indicates that, in contrast to our initial hypothesis, the reactions shown in eq 1 involve the initial hydrogenation of the isopropenyl group of the phosphine and that the *ortho*-CH activation of the aromatic ketones takes place on the 14-valence-electron monohydride $OsH(SnPh_2Cl)(P^iPr_3)_2$.

On the basis of the experimental results, a theoretical study on the reaction pathway for the hydrogenation of the isopropenyl group in the complex $OsH_3\{Sn(CH{=}CH_2)_2Cl\}\{\eta^2\text{-}CH_2{=}C(CH_3)PH_2\}(PH_3)$ (**1t**) was performed (Figure 4). The hydrogenation of the isopropenyl group is supposed to take place in two steps. In the first step, the double bond inserts into one of the Os−H bonds. In the second step, there is a reductive elimination of the resulting alkyl group and one of the two remaining hydrides, leading to a 14-valence-electron complex.

There are six potential intermediates for the insertion since we have three Os−H bonds in which the carbon−carbon double bond could insert. These hydrides could bond either to the terminal carbon atom of the double bond (C1) or to that bonded to the phosphorus atom (C2). Nevertheless, this number of possibilities can be reduced taking into account both that the formal insertion of C1 into the bonds Os−H1 and Os−H2 would lead to the same intermediate (**A**) and that the formal insertion of C2 into the bonds Os−H1 and Os−H2 would lead to intermediate **B**. The formal insertion of C2 into the Os−H3 bond would lead to intermediate **C**, whereas the formal insertion of C1 into the Os−H3 bond is highly unlikely due to the long distance between them (3.577

(25) Esteruelas, M. A.; Lledós, A.; Martín, M.; Maseras, F.; Osés, R.; Ruiz, N.; Tomàs, J. *Organometallics* **2001**, *20*, 5297.

Å) and to their geometrical disposition. Therefore, there are three feasible intermediates for this initial step. The calculated energies for each of these intermediates, **A**, **B**, and **C**, are 12.6, 21.8, and 26.1 kcal·mol^{-1} above **1t**, respectively. The most stable intermediate, **A**, presents a distorted octahedral geometry, with the phosphines in *trans* and the hydrides in *cis* positions, respectively. The other two intermediates have one phosphine *trans* to the stannyl ligand and the other phosphine *trans* to the carbon atom of the double bond.

To know the energy barrier for the first step, the transition state (**TS1**) connecting **1t** with intermediate **A** was located. We chose this pathway because the formal insertion of C1 into the Os−H1 bond corresponds to the easiest hydride motion; furthermore, this pathway leads to the most stable intermediate, **A**. The energy of **TS1** is 22.9 kcal·mol^{-1} above **1t**, and the Os−H1 and C1−H1 bond-breaking and bond-forming distances are 1.770 and 1.414 Å, respectively.

Once the reaction reaches the first intermediate, **A**, there is a reductive elimination of either H2 or H3 and the formed alkyl group. Each one of these pathways leads to a different intermediate, **D** or **E**. These intermediates are 14-valence-electron complexes, having a butterfly coordination mode with the phosphines in *trans* position. The energies of these intermediates are 9.6 and 8.5 kcal·mol^{-1} with regard to **1t**, respectively. The butterfly coordination mode of this intermediate makes it appropriate to undergo the subsequent C−H activation of the aromatic ketones or aromatic imines.

The calculated transition state for the second step (**TS2**) is the one connecting intermediates **A** and **D**. It corresponds to the reductive elimination of H2 and the formed alkyl group. Once again, this transition state corresponds to the hydride easiest motion. The energy of **TS2** is 29.5 kcal·mol^{-1} above **1t**. The forming C−H bond distance is 1.600 Å, whereas the breaking Os−H distance is 1.706 Å.

In summary, the hydrogenation of the isopropenyl group takes place in two steps. In the first one, the double bond inserts into the Os−H1 bond, with an energy barrier of 22.9 kcal·mol^{-1}. This insertion gives intermediate **A**, with an energy of 12.6 kcal·mol^{-1} above **1t**. In the second step, the reductive elimination of the hydride H2 and the formed alkyl group takes place. The energy of the transition state for this process is 29.5 kcal·mol^{-1}. This second step leads to an intermediate formally represented as a 14-valence-electron complex.[26] The high stability of this intermediate is remarkable, being more stable (∼11.5 kcal·mol^{-1}) than the 16-valence-electron complex resulting from the release of the double bond of the coordination sphere of the osmium atom in **1t**, which is located 21.1 kcal·mol^{-1} above **1t**.

3. Reactions with Partially Fluorinated Aromatic Ketones. Treatment at room temperature of toluene solutions of **1** with 1.5 equiv of 2,3,4,5,6-pentafluorobenzophenone and 2-fluoroacetophenone affords after several days red solutions, from which the compounds $OsH_2(SnPh_2Cl)\{C_6H_4C(O)C_6F_5\}(P^iPr_3)_2$ (**4**) and $OsH_2(SnPh_2Cl)\{C_6H_3FC(O)CH_3\}(P^iPr_3)_2$ (**5**) were isolated as red solids in about 65% yield. Complexes **4** and **5** (Scheme 1) are the result of the selective *ortho*-CH activation in the presence of *ortho*-CF bonds.

Scheme 1

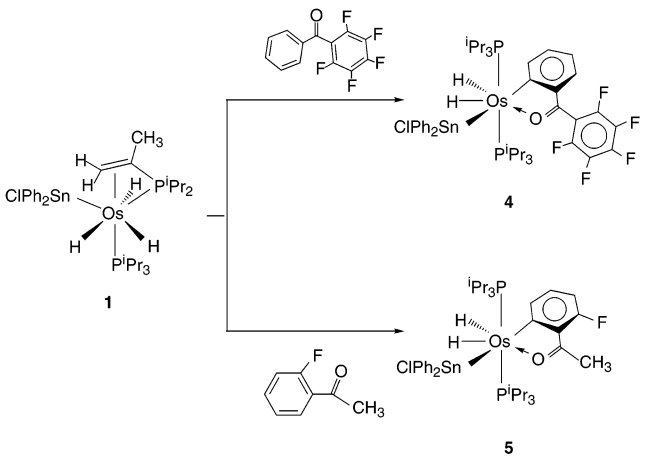

The behavior of **1** toward 2,3,4,5,6-pentafluorobenzophenone is in contrast to that previously observed for the d^2 hexahydride $OsH_6(P^iPr_3)_2$. In agreement with the *ortho*-CF activation of this ketone with the hexahydride, theoretical calculations for aromatic ketones suggest that in the presence of $OsH_6(P^iPr_3)_2$ the C−F activation is much more favored than the C−H activation, from a thermodynamic point of view. Although the C−F bonds are about 30 kcal·mol^{-1} stronger than the C−H bonds,[27] the higher energy required to break the C−F bond is largely compensated by the greater H−F bond energy compared with the H−H bond energy. The fact that the activation process with **1** does not involve the formation of any H−F bond can explain why with this complex the *ortho*-CH activation of 2,3,4,5,6-pentafluorobenzophenone, and in general the *ortho*-CH activation of any partially fluorinated aromatic ketone, is favored over the *ortho*-CF activation.

The behavior of **1** toward 2-fluoroacetophenone is similar to that of the d^2 hexahydride $OsH_6(P^iPr_3)_2$. To explain the origin of the selective *ortho*-CH activation with the hexahydride, it has been argued that the *ortho*-CH activation of 2-fluoroacetophenone has kinetic preference, which is related with the preferred *anti*-arrangement of the F−C−C−C=O unit.[9]

The activation of the C_6H_5 group of 2,3,4,5,6-pentafluorobenzophenone instead of the C_6F_5 is strongly supported by the ^{19}F NMR spectrum of **4** in benzene-d_6 at room temperature, which shows the typical three resonances of a C_6F_5 group at −136.6 (m, *o*-F), −149.5 (t, *p*-F), and −160.9 (m, *m*-F) ppm. The ^{19}F NMR spectrum of **5** also supports the *ortho*-CH activation of 2-fluoroacetophenone, showing a multiplet centered at −109.8 ppm. The IR and ^{1}H, ^{31}P{^{1}H}, ^{13}C{^{1}H}, and ^{119}Sn{^{1}H} NMR spectra of **4** and **5** are consistent with

(26) (a) Huang, D.; Streib, W. E.; Eisenstein, O.; Caulton, K. G. *Angew. Chem., Int. Ed. Engl.* **1997**, *36*, 2004. (b) Cooper, A. C.; Streib, W. E.; Eisenstein, O.; Caulton, K. G. *J. Am. Chem. Soc.* **1997**, *119*, 9069. (c) Huang, D.; Streib, W. E.; Bollinger, J. C.; Caulton, K. G.; Winter, R. F.; Scheiring, T. *J. Am. Chem. Soc.* **1999**, *121*, 8087. (d) Huang, D.; Bollinger, J. C.; Streib, W. E.; Folting, K.; Young, V., Jr.; Eisenstein, O.; Caulton, K. G. *Organometallics* **2000**, *19*, 2281. (e) Tamm, M.; Dressel, B.; Lügger, T.; Fröhlich, R.; Grimme, S. *Eur. J. Inorg. Chem.* **2003**, 1088.

(27) Smart, B. E. In *The Chemistry of Functional Groups, Supplement D*; Patai, S., Rappoport, Z., Eds.; John Wiley and Sons: Chichester, 1983; Chapter 14.

the structures proposed for these compounds in Scheme 1 and agree well with those of **2** and **3**.

The IR spectra contain the ν(Os−H) and ν(C═O) bands at 2236 (**4**) and 2086 (**5**) cm^{-1}, and 1652 (**4**) and 1603 (**5**) cm^{-1}, respectively.

The ^1H NMR spectra are temperature-dependent. At 333 K in toluene as solvent, the spectrum of **4** shows in the hydride region a broad resonance centered at −11.11 ppm. At about 293 K decoalescence occurs, and at 233 K an ABX_2 spin system defined by $\delta_A = -10.12$, $\delta_B = -12.50$, $J_{A-B} = 25$ Hz, $J_{A-X} = 11.7$ Hz, and $J_{B-X} = 15$ Hz is observed. The behavior of the spectra of **5** with the temperature is similar. At 303 K the hydride ligands give rise to a broad resonance centered at −11.66 ppm. At about 273 K, decoalescence occurs, and at 233 K, the ABX_2 spin system is observed. In this case, the ABX_2 spin system is defined by the parameters $\delta_A = -10.65$, $\delta_B = -12.70$, $J_{A-B} = 59$ Hz, $J_{A-X} = 8.3$ Hz, and $J_{B-X} = 12.5$ Hz. The rate constants for the exchange of the hydrides were calculated from the $^1H\{^{31}P\}$ NMR spectra at each temperature, for both compounds (Table 3). The activation parameters obtained are $\Delta H^{\ddagger} = 12.6 \pm 0.5$ kcal·mol^{-1} and $\Delta S^{\ddagger} = -2.9 \pm 1$ cal·mol^{-1}·K^{-1} (**4**) and $\Delta H^{\ddagger} = 11.2 \pm 0.4$ kcal·mol^{-1} and $\Delta S^{\ddagger} = -2.8 \pm 1.1$ cal·mol^{-1}·K^{-1} (**5**). The T_1 values of the hydride resonances of these compounds were also determined, in this case, over the temperature range 293−213 K. $T_{1(min)}$ values of 85 ± 2 (**4**) and 79 ± 4 (**5**) ms were found at 248 K. They lead to a separation between the hydride ligands of **4** and **5** of about 1.5 Å.

Like the $^{31}P\{^1H\}$ NMR of **2** and **3**, the $^{31}P\{^1H\}$ NMR spectra of **4** and **5** are also temperature-dependent. At 293 K, the spectrum of **4** shows a singlet at 8.4 ppm, along with the tin satellites ($J_{P-^{119}Sn} = J_{P-^{117}Sn} = 114$ Hz). At 183 K, the singlet is converted into an AB spin system centered at 6.8 ppm and defined by $\Delta\nu = 863$ Hz and $J_{A-B} = 197$ Hz. At 293 K, the singlet of **5** appears at 7.1 ppm and the P−^{119}Sn and P−^{117}Sn coupling constants are 115 Hz. At 183 K, the AB spin system is observed at 6.1 ppm and is defined by $\Delta\nu = 705$ Hz and $J_{A-B} = 203$ Hz.

In the $^{13}C\{^1H\}$ NMR spectrum of **4** at room temperature, the resonance corresponding to the CO-carbon atom of the ketone appears at 203.4 ppm, whereas the resonance due to the metalated carbon atom is observed at 194.0 ppm. In the spectrum of **5**, the carbonyl resonance appears at 210.6 ppm, whereas the metalated resonance is observed at 198.7 ppm. At room temperature, the $^{119}Sn\{^1H\}$ NMR spectrum of **4** shows a triplet at 7.9 ppm, whereas the $^{119}Sn\{^1H\}$ NMR spectrum of **5** contains a double triplet at 12.3 ppm, with a ^{119}Sn−F coupling constant of 41 Hz.

4. Activation of Benzophenone Imine. Complex **1** is capable of activating not only aromatic ketones and partially fluorinated aromatic ketones but also aromatic imines. Thus, treatment at room temperature of toluene solutions of **1** with 1.5 equiv of benzophenone imine leads after 40 h to orange solutions, from which the orthometalated benzophenone imine derivative $OsH_2(SnPh_2Cl)\{C_6H_4C(NH)C_6H_5\}(P^iPr_3)_2$ (**6**) is obtained as an orange solid in almost quantitative yield. The formation of **6** (eq 3) is a process similar to those described for the ketones, involving the reduction of the isopropenyl group of the isopropenylphosphine of **1** and the *ortho*-CH activation of one of the phenyl groups of the imine.

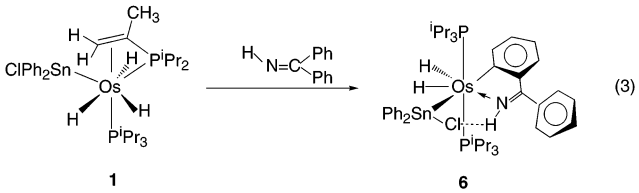

1 **6** (3)

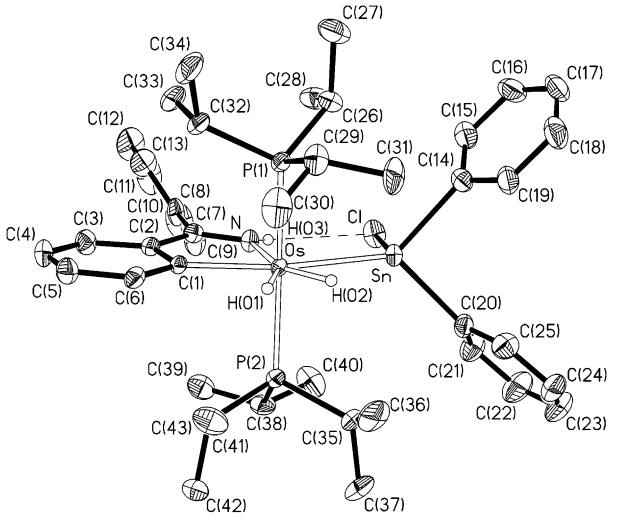

Figure 5. Molecular diagram of the complex $OsH_2(SnPh_2Cl)\{C_6H_4C(NH)C_6H_5\}(P^iPr_3)_2$ (**6**).

Table 4. Selected Bond Distances (Å) and Angles (deg) for the Complex $OsH_2(SnPh_2Cl)\{C_6H_4C(NH)C_6H_5\}(P^iPr_3)_2$ (6)

Os−Sn	2.7004(4)	Sn−H(02)	1.43(4)
Os−P(1)	2.3846(11)	Sn−Cl	2.4503(11)
Os−P(2)	2.3694(10)	N−C(7)	1.295(5)
Os−N	2.094(3)	C(1)−C(2)	1.403(5)
Os−C(1)	2.108(4)	C(2)−C(7)	1.442(5)
Os−H(01)	1.53(6)	Cl···H(03)	2.59

Sn−Os−P(1)	93.92(3)	P(2)−Os−H(02)	84.9(16)
Sn−Os−P(2)	94.39(3)	N−Os−C(1)	74.68(14)
Sn−Os−N	84.71(9)	N−Os−H(01)	153(2)
Sn−Os−C(1)	159.35(11)	N−Os−H(02)	149.9(16)
Sn−Os−H(01)	122(1)	C(1)−Os−H(01)	78(2)
Sn−Os−H(02)	65.2(16)	C(1)−Os−H(02)	135.4(16)
P(1)−Os−P(2)	161.14(4)	H(01)−Os−H(02)	57(2)
P(1)−Os−N	98.66(10)	Os−Sn−Cl	106.60(3)
C(14)−Sn−Cl	95.29(13)	C(14)−Sn−C(20)	94.06(16)
Os−Sn−C(14)	127.34(11)	Os−Sn−C(20)	128.10(11)
C(20)−Sn−Cl	97.67(12)	P(1)−Os−C(1)	88.09(10)
Os−N−C(7)	121.1(3)	P(1)−Os−H(01)	81(2)
Os−C(1)−C(2)	115.8(3)	P(1)−Os−H(02)	83.2(16)
N−C(7)−C(8)	121.8(4)	P(2)−Os−N	98.95(10)
C(2)−C(7)−C(8)	124.3(4)	P(2)−Os−C(1)	90.07(10)
C(1)−C(2)−C(7)	114.5(3)	P(2)−Os−H(01)	80(2)

A view of the molecular geometry of **6** is shown in Figure 5. Selected bond distances and angles are listed in Table 4. The coordination geometry around the osmium atom is similar to that of **2** and can be rationalized as a distorted pentagonal bipyramid with the two phosphorus atoms of the triisopropylphosphine ligands occupying axial positions (P(2)−Os−P(1) = 161.14(4)°). The osmium sphere is completed by the orthometalated imine, which acts with a bite angle of

74.68(14)°, the stannyl ligand *cisoid* disposed to the nitrogen atom of the imine (84.71(9)°), and the hydride ligands.

The five-membered ring formed by the metalated imine and the osmium atom is almost planar. The Os−N bond length of 2.094(3) Å and the Os−C(1) bond distance of 2.108(4) Å are typical for Os−N and Os−C(aryl) single bonds, respectively, and are in agreement with the values previously found for the complexes $[OsH(\eta^5\text{-}C_5H_5)\{C_6H_4C(NH)C_6H_5\}(P^iPr_3)]BF_4$ (2.078(18) and 2.080(19) Å, and 2.10(2) and 2.137(19) Å),[13a] $OsCl\{C_6H_4C(NH)C_6H_5\}(\eta^2\text{-}H_2)(P^iPr_3)_2$ (2.097(3) and 2.069(4) Å),[19f] $Os(C_2Ph)\{C_6H_4C(NH)C_6H_5\}(CO)(P^iPr_3)_2$ (2.106(7) and 2.089(7) Å),[13a] $[Os\{C_6H_4C(NH)C_6H_5\}(\eta^6\text{-}C_6H_3Me_3)(P^iPr_3)]PF_6$ (2.083(4) and 2.072(4) Å),[28] $OsH\{(C_6H_3\text{-}p\text{-}Me)(p\text{-tolyl})CNNC(p\text{-tolyl})_2\}(CO)_2(PPh_3)$ (2.119(5) and 2.100(7) Å),[29] and *fac*-Os{*C*,*N*-3-Me[2-(MeC_6H_4)NCMe_2]-C_6H_3}(2-MeC_6H_4)(CN-^{t}Bu)$_3$ (2.193(24) and 2.077(20) Å).[30] The N−C(7) distance of 1.295(5) Å is similar to those observed in imine transition metal complexes,[31] azavinylidene compounds,[32] organic azaallenium cation,[33] and 2-azaallenyl complexes.[34]

The Os−Sn distance (2.7004(4) Å) is statistically identical with the Os−Sn bond length found in **2**. As in the latter, the environment of the tin atom is tetrahedral, with the chlorine atom lying in the equatorial plane of the bipyramid and the C−Sn−C angle strongly deviated from the ideal value of 109° (C(14)−Sn−C(20) = 94.06(16)°). The Sn−Cl distance (2.4503(11) Å) is about 0.02 Å longer than those found in **1** (2.432(3) Å) and **2** (2.4331(14) Å). Interestingly, the separation between the chlorine and the hydrogen atom (H(03)) of the imine (2.59 Å) is shorter than the sum of the van der Waals radii of hydrogen and chlorine [r_{vdw}(H) = 1.20, r_{vdw}(Cl) = 1.80 Å],[35] suggesting that there is an intramolecular Cl···H−N hydrogen bond, as a result of the electrostatic interaction of the electronegative chlorine and the acidic NH hydrogen of the imine. Of great importance in biological and organic chemistry,[36] the hydrogen bonding is presently attracting considerable interest in the chemistry of transition metals.[31,37]

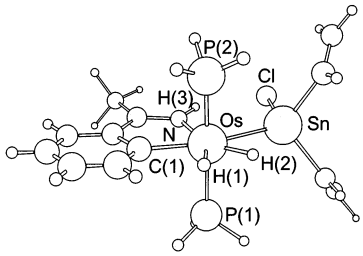

Figure 6. B3LYP optimized structure of the model complex $OsH_2\{Sn(CH{=}CH_2)_2Cl\}\{C_6H_4C(NH)CH_3\}(PH_3)_2$ (**6t**).

Table 5. Optimized (B3LYP) Distances (Å) and Angles (deg) of $OsH_2\{Sn(CH{=}CH_2)_2Cl\}\{C_6H_4C(NH)CH_3\}(PH_3)_2$ (6t)

Os−Sn	2.717	Os−P(1)	2.333
Os−P(2)	2.333	Os−N	2.148
Os−C(1)	2.139	N−H(3)	1.022
Os−H(1)	1.645	Os−H(2)	1.671
Sn−Cl	2.519	Cl···H(3)	2.400
H(1)···H(2)	1.706	Sn···H(2)	2.395
Sn−Os−P(1)	92.434	Sn−Os−P(2)	92.287
N−Os−P(1)	92.926	N−Os−P(2)	92.754
C(1)−Os−P(1)	88.605	C(1)−Os−P(2)	88.806
Sn−Os−N	84.837	Sn−Os−C(1)	159.613
N−Os−C(1)	74.774	P(1)−Os−P(2)	172.919
H(1)−Os−Sn	122.647	H(2)−Os−Sn	60.723
H(1)−Os−P(1)	86.466	H(2)−Os−P(1)	88.853
H(1)−Os−P(2)	86.542	H(2)−Os−P(2)	88.855
H(1)−Os−N	152.515	H(2)−Os−N	145.561
H(1)−Os−C(1)	77.740	H(2)−Os−C(1)	139.664
H(1)−Os−H(2)	61.924		

To corroborate the structure of **6**, a DFT study of the model complex $OsH_2\{Sn(CH{=}CH_2)_2Cl\}\{C_6H_4C(NH)CH_3\}(PH_3)_2$ (**6t**) was also carried out. Figure 6 shows the B3LYP optimized structure of **6t**, whereas its main geometrical parameters are collected in Table 5. Theoretical results are consistent with the presence of an intramolecular Cl···H−N hydrogen bond and support the dihydride character of the complex. The separation between the chlorine bonded to the tin atom and the hydrogen of the imine (H(3)) is 2.40 Å. As for **2t**, the Os−H distances are about 1.6 Å and the separation between the hydride ligands is 1.706 Å. Neither, in this case, is there interaction between the tin atom and the hydride ligand disposed *cisoid* to it. The separation between them is 2.395 Å.

The intramolecular Cl···H−N hydrogen bond is also supported by the IR spectrum of **6** in Nujol, which shows the N−H stretching frequency at 3246 cm^{-1}, shifted 83

(28) Werner, H.; Daniel, T.; Braun, T.; Nürnberg, O. *J. Organomet. Chem.* **1994**, *480*, 145.
(29) Gallop, M. A.; Rickard, C. E. F.; Roper, W. R. *J. Organomet. Chem.* **1990**, *395*, 333.
(30) Arnold, J.; Wilkinson, G.; Hussain, B.; Hursthouse, M. B. *Organometallics* **1989**, *8*, 1362.
(31) Castarlenas, R.; Esteruelas, M. A.; Gutiérrez-Puebla, E.; Oñate, E. *Organometallics* **2001**, *20*, 1545, and references therein.
(32) Castarlenas, R.; Esteruelas, M. A.; Jean, Y.; Lledós, A.; Oñate, E.; Tomàs, J. *Eur. J. Inorg. Chem.* **2001**, *2871*, and references therein.
(33) See for example: (a) Jochims, J. C.; Abu-El-Halawa, R.; Jibril, I.; Huttner, G. *Chem. Ber.* **1984**, *117*, 1900. (b) Al-Talib, M.; Jochims, J. C. *Chem. Ber.* **1984**, *117*, 3222. (c) Al-Talib, M.; Jibril, I.; Würthwein, E.-U.; Jochims, J. C.; Huttner, G. *Chem. Ber.* **1984**, *117*, 3365. (d) Kupfer, R.; Würthwein, E.-U.; Nagel, M.; Allmann, R. *Chem. Ber.* **1985**, *118*, 643. (e) Al-Talib, M.; Jibril, I.; Huttner, G.; Jochims, J. C. *Chem. Ber.* **1985**, *118*, 1876. (f) Al-Talib, M.; Jochims, J. C.; Zsolnai, L.; Huttner, G. *Chem. Ber.* **1985**, *118*, 1887. (g) Würthwein, E.-U.; Kupfer, R.; Allmann, R.; Nagel, M. *Chem. Ber.* **1985**, *118*, 3632. (h) Krestel, M.; Kupfer, R.; Allmann, R.; Würthwein, E.-U. *Chem. Ber.* **1987**, *120*, 1271.
(34) (a) Seitz, F.; Fischer, H.; Riede, J. *J. Organomet. Chem.* **1985**, *287*, 87. (b) Aumann, R.; Atlhaus, S.; Krüger, C.; Betz, P. *Chem. Ber.* **1989**, *122*, 357. (c) Esteruelas, M. A.; Gómez, A. V.; Lahoz, F. J.; López, A. M.; Oñate, E.; Oro, L. A. *Organometallics* **1996**, *15*, 3423.
(35) Bondi, A. *J. Phys. Chem.* **1964**, *68*, 441.
(36) Jeffrey, G. A.; Saenger, W.; *Hydrogen Bonding in Biological Structures*; Springer: Berlin, 1991.
(37) See for example: (a) Stevens, R. C.; Bau, R.; Milstein, D.; Blum, O.; Koetzle, T. F. *J. Chem. Soc., Dalton Trans.* **1990**, *1429*. (b) Lough, A. J.; Park, S.; Ramachandran, R.; Morris, R. H. *J. Am. Chem. Soc.* **1994**, *116*, 8356. (c) Peris, E.; Lee, J. C. L., Jr.; Rambo, J. R.; Eisenstein, O.; Crabtree, R. H. *J. Am. Chem. Soc.* **1995**, *117*, 3485. (d) Crabtree, R. H.; Eisenstein, O.; Sini, G.; Peris, E. *J. Organomet. Chem.* **1998**, *567*, 7. (e) Crabtree, R. H. *J. Organomet. Chem.* **1998**, *557*, 111. (f) Gusev, D. G.; Lough, A. J.; Morris, R. H. *J. Am. Chem. Soc.* **1998**, *120*, 13138. (g) Buil, M. L.; Esteruelas, M. A.; Oñate, E.; Ruiz, N. *Organometallics* **1998**, *17*, 3346. (h) Esteruelas, M. A.; Oliván, M.; Oñate, E.; Ruiz, N.; Tajada, M. A. *Organometallics* **1999**, *18*, 2953. (i) Lee, D.-H.; Kwon, H. J.; Patel, B. P.; Liable-Sands, L. M.; Rheingold, A. L.; Crabtree, R. H. *Organometallics* **1999**, *18*, 1615. (j) Clot, E.; Eisenstein, O.; Crabtree, R. H. *New J. Chem.* **2001**, *25*, 66. (k) Barrio, P.; Esteruelas, M. A.; Oñate, E. *Organometallics* **2002**, *21*, 2491.

cm^{-1} to lower wavenumbers in comparison with that observed in the complex $Os(C_2Ph)\{C_6H_4C(NH)C_6H_5\}(CO)(P^iPr_3)_2$ (3329 cm^{-1})[13a] and between 100 and 60 cm^{-1} with regard to those found in the compounds $OsH_2X\{C_6H_4C(NH)C_6H_5\}(P^iPr_3)_2$ (X = H, Cl, Br, I, between 3348 and 3300 cm^{-1}).[19f] In addition, the ν(Os−H) and ν(C═N) bands, which appear at 2077 and 1579 cm^{-1}, respectively, should be mentioned.

In toluene-d_8 and benzene-d_6, the Cl···H−N interaction seems to be retained. Thus, the ^{1}H NMR spectra in these solvents show the NH resonance at about 12.8 ppm, shifted about 2 ppm toward lower field with regard to the chemical shift found for the resonance of the complexes $OsH_2X\{C_6H_4C(NH)C_6H_5\}(P^iPr_3)_2$ (between 10.2 and 10.8 ppm).[19f] In this context, the presence of tin satellites around the NH resonance ($J_{H-^{119}Sn} = J_{H-^{117}Sn} = 77$ Hz) of **6** should also be pointed out. In the high-field region, the spectra show the hydride resonance. In toluene-d_8, at 293 K, it appears as a triplet at −9.79 ppm with a H−P coupling constant of 14.4 Hz. Lowering the sample temperature produces a broadening of this resonance. Between 203 and 193 K, its decoalescence starts to be observed. The T_1 values were determined over the temperature range 293−213 K. A $T_{1(min)}$ value of 81 ± 1 ms was found at 243 K. It leads to a separation between the hydride ligands of about 1.5 Å.

The $^{31}P\{^1H\}$ NMR spectrum in toluene-d_8 at 293 K contains a singlet at 2.7 ppm, along with the tin satellites ($J_{P-^{119}Sn} = J_{P-^{117}Sn} = 107$ Hz). Lowering the sample temperature leads to a broadening of the resonance. At 223 K decoalescence occurs. The spectrum at 183 K shows an AB spin system centered at 3.7 ppm and defined by $\Delta\nu = 879$ Hz and $J_{A-B} = 202$ Hz, and a singlet at −0.8 ppm. The presence of two resonances in this spectrum suggests that, in this case, the resistance to the rotation around the Os−P or/and Os−Sn bonds gives rise to an equilibrium mixture of two conformers of **6**, one of them containing equivalent phosphines and the other one containing inequivalent phosphine ligands. It should be noted that the presence of the Cl···H−N hydrogen bond increases the resistance to the rotation around the Os−Sn bond.

In the $^{13}C\{^1H\}$ NMR spectrum, at room temperature, the most noticeable resonances are two triplets at 181.3 and 178.1 ppm, with C−P coupling constants of 2 and 8 Hz, which were assigned to the C═N and metalated carbon atoms of the imine, respectively. At this temperature, the $^{119}Sn\{^1H\}$ NMR spectrum shows a triplet at 0.3 ppm.

The chlorine bonded to the tin atom of **6** can be replaced by a hydroxy group. Thus, the treatment of tetrahydrofuran solutions of **6** with 1.1 equiv of KOH, for 2 days at room temperature, affords the stannahydroxy derivative $OsH_2(SnPh_2OH)\{C_6H_4C(NH)C_6H_5\}(P^iPr_3)_2$ (**7**), which was isolated as an orange solid in 78% yield, according to eq 4.

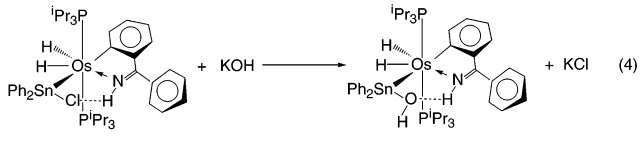

6 **7** (4)

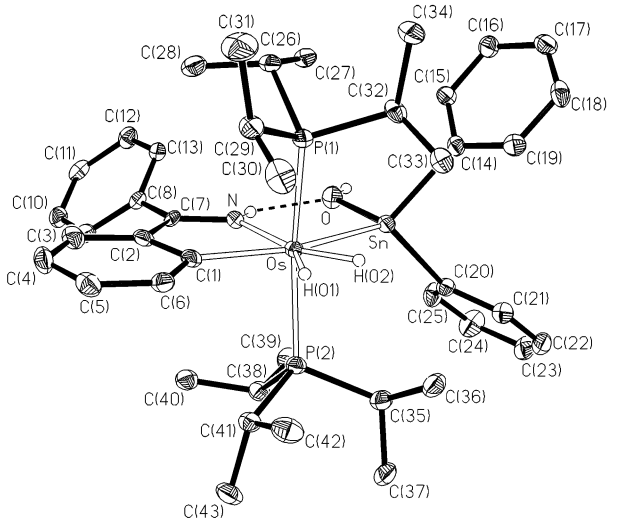

Figure 7. Molecular diagram of the complex $OsH_2(SnPh_2OH)\{C_6H_4C(NH)C_6H_5\}(P^iPr_3)_2$ (**7**).

Table 6. Selected Bond Distances (Å) and Angles (deg) for the Complex $OsH_2(SnPh_2OH)\{C_6H_4C(NH)C_6H_5\}(P^iPr_3)_2$ (7)

Os−Sn	2.6908(4)	Sn−H(02)	1.58(6)
Os−P(1)	2.3858(14)	Sn−O	2.031(5)
Os−P(2)	2.3720(14)	N−C(7)	1.309(7)
Os−N	2.102(5)	C(1)−C(2)	1.418(8)
Os−C(1)	2.114(5)	C(2)−C(7)	1.442(8)
Os−H(01)	1.68(6)	O···H(04)	2.052
Sn−Os−P(1)	94.42(4)	P(2)−Os−H(02)	85(2)
Sn−Os−P(2)	93.05(4)	N−Os−C(1)	74.9(2)
Sn−Os−N	81.06(13)	N−Os−H(01)	157(2)
Sn−Os−C(1)	155.92(16)	N−Os−H(02)	156(2)
Sn−Os−H(01)	122(2)	C(1)−Os−H(01)	82(2)
Sn−Os−H(02)	75(2)	C(1)−Os−H(02)	129(2)
P(1)−Os−P(2)	162.84(5)	H(01)−Os−H(02)	46(3)
P(1)−Os−N	97.45(13)	Os−Sn−O	101.46(14)
Os−Sn−C(14)	126.84(14)	Os−Sn−C(20)	130.55(14)
C(14)−Sn−C(20)	93.81(19)	C(14)−Sn−O	99.7(2)
C(20)−Sn−O	97.1(2)	P(1)−Os−C(1)	89.62(14)
Os−N−C(7)	121.3(4)	P(1)−Os−H(01)	80(2)
Os−C(1)−C(2)	115.4(4)	P(1)−Os−H(02)	82(2)
N−C(7)−C(8)	119.9(5)	P(2)−Os−N	98.95(13)
C(2)−C(7)−C(8)	126.7(5)	P(2)−Os−C(1)	89.84(14)
C(1)−C(2)−C(7)	115.0(5)	P(2)−Os−H(01)	83(2)

Complex **7** is a rare example of a monomeric stannahydroxy compound.[15b,38] In general, hydroxy, thiahydroxy, and selenahydroxy functionalities tend to form polymeric structures following condensation reactions.[39]

A view of the molecular geometry of **7** is shown in Figure 7. Selected bond distances and angles are listed in Table 6. The structure of **7** is similar to that of **6**. The most noticeable feature is the presence of an intramolecular O···H−N hydrogen bond between the oxygen atom of the hydroxy group and the hydrogen of the imine. The separation between these atoms (2.052 Å) is about 0.55 Å shorter that the sum of the van der Waals radii of hydrogen and oxygen (r_{vdw}(H) = 1.20 Å;

(38) Vicente, J.; Chicote, M. T.; Ramírez-de-Arellano, M.-del-C.; Jones, P. G. *J. Chem. Soc., Dalton Trans.* **1992**, 1839.

(39) See for example: (a) Reuter, H.; Puff, H. *J. Organomet. Chem.* **1989**, *379*, 223. (b) Puff, H.; Reuter, H. *J. Organomet. Chem.* **1989**, *368*, 173. (c) Puff, H.; Reuter, H. *J. Organomet. Chem.* **1989**, *364*, 57.

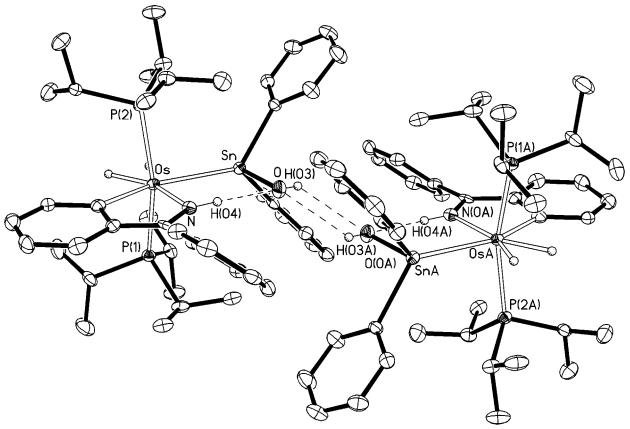

Figure 8. Intramolecular O···H−N and intermolecular O···H−O interactions in $OsH_2(SnPh_2OH)\{C_6H_4C(NH)C_6H_5\}(P^iPr_3)_2$ (**7**).

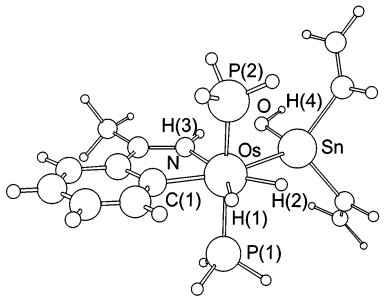

Figure 9. B3LYP optimized structure of the model complex $OsH_2\{Sn(CH{=}CH_2)_2(OH)\}\{C_6H_4C(NH)CH_3\}(PH_3)_2$ (**7t**).

$r_{vdw}(O) = 1.40$ Å).[35] An extended view of the structure (Figure 8) indicates also short intermolecular interactions (2.439 Å) between the oxygen and O−H hydrogen atoms of two adjacent molecules in the crystal.

The structure of **7** was corroborated by a DFT study of the model complex $OsH_2\{Sn(CH{=}CH_2)_2(OH)\}\{C_6H_4C(NH)CH_3\}(PH_3)_2$ (**7t**). Figure 9 shows the B3LYP optimized structure of **7t**, whereas the main geometrical parameters are collected in Table 7. The theoretical results are also consistent with the presence of the intramolecular O···H−N hydrogen bond. In agreement with the X-ray diffraction results, the separation between the oxygen atom and the hydrogen of the imine (H(3)) is 1.92 Å.

The hydrogen bond in **7** is stronger than in **6**. Thus, in the IR spectrum of **7** in Nujol, the ν(N−H) band appears at 3167 cm^{-1}, shifted 79 cm^{-1} to lower wavenumbers in comparison with that observed in **6**. In agreement with the IR spectra, the ^1H NMR spectrum of **7** in toluene-d_8 at room temperature shows the NH resonance at 14.07 ppm, shifted about 2 ppm toward lower field with regard to the chemical shift observed for the N−H resonance of **6**. Tin satellites around the NH resonance of **7** are also observed ($J_{H-^{119}Sn} = J_{H-^{117}Sn} = 75$ Hz).

In addition to the NH resonance, the OH and hydride resonances should be mentioned. In toluene at room temperature, the OH resonance is observed as a broad singlet at 0.65 ppm, along with the tin satellites ($J_{H-^{119}Sn} = J_{H-^{117}Sn} = 34$ Hz). The presence of only one $J_{H-^{119}Sn}$ (or $J_{H-^{117}Sn}$) coupling constant suggests that the intermolecular O···H−O hydrogen bond is broken in solution. The hydride resonance appears as a broad signal at −9.90 ppm. The behavior of the hydride resonance with the temperature is similar to that observed for the hydride resonance of **6**. The T_1 values were determined over the temperature range 263−223 K. A $T_{1(min)}$ value of 84 ± 6 ms was found at 243 K. It leads to a separation between the hydride ligands of about 1.5 Å, suggesting that the replacement of the chlorine by the hydroxy group has no significant influence on the interactions within the OsH_2 unit. In agreement with this, the separation between the hydride ligands of **7t** (1.740 Å) is similar to that found in **6t**.

The $^{31}P\{^1H\}$ NMR spectrum in toluene at room temperature contains a singlet at 5.1 ppm, along with the tin satellites ($J_{P-^{119}Sn} = J_{P-^{117}Sn} = 108$ Hz). At 183 K, the spectrum shows an AB spin system centered at 2.9 ppm and defined by $\Delta\nu = 1094$ Hz and $J_{AB} = 237$ Hz, and a singlet at −0.1 ppm. In the $^{13}C\{^1H\}$ NMR spectrum at room temperature the resonances corresponding to the C=N and metalated carbon atoms of the imine are observed as triplets at 180.2 and 180.0 ppm, with C−P coupling constants of 2 and 8 Hz, respectively. At this temperature, the $^{119}Sn\{^1H\}$ NMR spectrum contains a triplet at −98.1 ppm.

Table 7. Optimized (B3LYP) Distances (Å) and Angles (deg) of $OsH_2\{Sn(CH{=}CH_2)_2(OH)\}\{C_6H_4C(NH)CH_3\}(PH_3)_2$ (7t)

Os−Sn	2.711	Os−P(1)	2.326
Os−P(2)	2.327	Os−N	2.151
Os−C(1)	2.136	Sn−O	1.993
Os−H(1)	1.649	Os−H(2)	1.670
N−H(3)	1.026	O−H(4)	0.967
O···H(3)	1.92	H(1)···H(2)	1.740
Sn···H(2)	2.450		
Sn−Os−P(1)	92.600	Sn−Os−P(2)	91.955
N−Os−P(1)	92.990	N−Os−P(2)	93.814
C(1)−Os−P(1)	89.343	C(1)−Os−P(2)	89.109
Sn−Os−N	80.004	Sn−Os−C(1)	154.984
N−Os−C(1)	74.989	P(1)−Os−P(2)	172.379
H(1)−Os−Sn	126.072	H(2)−Os−Sn	62.826
H(1)−Os−P(1)	86.253	H(2)−Os−P(1)	88.395
H(1)−Os−P(2)	86.127	H(2)−Os−P(2)	88.255
H(1)−Os−N	153.925	H(2)−Os−N	142.825
H(1)−Os−C(1)	78.937	H(2)−Os−C(1)	142.185
H(1)−Os−H(2)	63.250		

Concluding Remarks

This paper reveals that the trihydride-stannyl complex $OsH_3(SnPh_2Cl)\{\eta^2\text{-}CH_2{=}C(CH_3)P^iPr_2\}(P^iPr_3)$ activates one *ortho*-CH bond of aromatic ketones, partially fluorinated aromatic ketones, and aromatic imines, under mild conditions. Thus, the reactions of this compound with acetophenone, benzophenone, 2,3,4,5,6-pentafluorobenzophenone, 2-fluoroacetophenone, and benzophenone imine afford the dihydride-stannyl derivatives $OsH_2(SnPh_2Cl)\{C_6H_4C(O)R\}(P^iPr_3)_2$ (R = CH_3, C_6H_5, C_6F_5), $OsH_2(SnPh_2Cl)\{C_6H_3FC(O)CH_3\}(P^iPr_3)_2$, and $OsH_2(SnPh_2Cl)\{C_6H_4C(NH)C_6H_5\}(P^iPr_3)_2$, respectively.

The activation process takes place on the 14-valence-electron monohydride $OsH(SnPh_2Cl)(P^iPr_3)_2$. This intermediate is generated from the starting complex, previous to the activation, by migration of two of the hydride ligands from the osmium atom to the isopropenyl group of one of the phosphines. DFT calculations show that this migration proceeds through a two-step process.

Spectroscopy studies, X-ray diffraction analysis, and DFT calculations indicate that, in all the cases, the formed products are classical dihydrides and that there is no interaction between the tin atom and any of the hydride ligands. On the other hand, for the complex $OsH_2(SnPh_2Cl)\{C_6H_4C(NH)C_6H_5\}(P^iPr_3)_2$, an intramolecular Cl···H−N hydrogen bond between the chlorine bonded to the tin atom and the hydrogen of the imine is detected. Substitution of the chlorine for a hydroxy group affords the monomeric stannahydroxy compound $OsH_2(SnPh_2OH)\{C_6H_4C(NH)C_6H_5\}(P^iPr_3)_2$, which shows intramolecular O···H−N and intermolecular O···H−O hydrogen bonds.

Experimental Section

All reactions were carried out under an argon atmosphere using Schlenk tube techniques. Solvents were dried and purified by known procedures and distilled under argon prior to use. The starting material $OsH_3(SnPh_2Cl)\{\eta^2\text{-}CH_2{=}C(CH_3)P\text{-}^iPr_2\}(P^iPr_3)$ (**1**) was prepared as previously described.[12] Infrared spectra were recorded on a Perkin-Elmer 883 spectrometer as solids (Nujol mull). ^1H, ^2H, $^{13}C\{^1H\}$, $^{31}P\{^1H\}$, ^{19}F, and $^{119}Sn\{^1H\}$ NMR spectra were recorded on either a Varian Gemini 2000, a Varian UNITY 300, or a Bruker AXR 300 instrument. Chemical shifts are referenced to residual solvent peaks (^1H, ^2H, and $^{13}C\{^1H\}$), external H_3PO_4 ($^{31}P\{^1H\}$), $CFCl_3$ (^{19}F), or Me_4Sn ($^{119}Sn\{^1H\}$). Coupling constants J and N ($N = J_{P-H} + J_{P'-H}$ for ^1H; $N = J_{P-C} + J_{P'-C}$ for $^{13}C\{^1H\}$) are given in hertz. C, H, and N analyses were measured on a Perkin-Elmer 2400 CHNS/O analyzer.

Preparation of $OsH_2(SnPh_2Cl)\{C_6H_4C(O)CH_3\}(P^iPr_3)_2$ (2). Acetophenone (30.3 μL, 0.260 mmol) was added to a solution of **1** (136 mg, 0.173 mmol) in toluene (10 mL). After stirring for 30 h at room temperature the color of the solution had changed to orange. The resulting solution was filtered through Celite and was taken to dryness. Subsequent addition of pentane caused the precipitation of an orange solid, which was washed with pentane and dried in vacuo. Yield: 116 mg (71%). Anal. Calcd for $C_{38}H_{61}ClOOsP_2Sn$: C, 48.55; H, 6.54. Found: C, 48.10; H, 6.52. IR (Nujol, cm^{-1}): ν(OsH) 2086 (w), ν(CO) 1590 (m). ^1H NMR (300 MHz, C_7D_8, 303 K): δ 8.20 (d, J_{H-H} = 7.2, 4H, SnPh−H_{ortho}), 8.03 (d, J_{H-H} = 7.5, 1H, Os−C_6H_4), 7.15 (t, J_{H-H} = 7.2, 4H, SnPh−H_{meta}), 7.08 (d, J_{H-H} = 7.5, 1H, Os−C_6H_4), 7.00 (t, J_{H-H} = 7.2, 2H, SnPh−H_{para}), 6.68 (t, J_{H-H} = 7.5 Hz, 1H, Os−C_6H_4), 6.53 (t, J_{H-H} = 7.5 Hz, 1H, Os−C_6H_4), 2.3 (s, 3H, CH_3), 2.00 (m, 6H, PCH(CH_3)$_2$), 0.80 (dvt, N = 13.5, J_{H-H} = 6.9, 18H, PCH(CH_3)$_2$), 0.51 (dvt, N = 13.5, J_{H-H} = 6.9, 18H, PCH(CH_3)$_2$), −11.86 (br, 2H, OsH). ^1H NMR (300 MHz, C_7D_8, 233 K, hydride region): δ −11.02 (part A of an ABX_2 spin system, 1H, J_{A-X} = 14, J_{A-B} = 46), −13.01 (part B of an ABX_2 spin system, 1H, J_{B-X} = 14, J_{A-B} = 46). $^{31}P\{^1H\}$ NMR (121.42 MHz, C_7D_8, 293 K): δ 7.4 (s with tin satellites $J_{P-^{117}Sn} = J_{P-^{119}Sn}$ = 113). $^{31}P\{^1H\}$ NMR (121.42 MHz, C_7D_8, 183 K): δ 6.9 (AB spin system, $\Delta\nu$ = 549 Hz, J_{A-B} = 202). $^{13}C\{^1H\}$ NMR (75.42 MHz, C_6D_6, 293 K): δ 212.7 (t, J_{P-C} = 2, CO), 194.9 (t, J_{P-C} = 7, OsC), 156.4 (s, C_{ipso}, $SnPh_2Cl$), 143.6 (s, Ph), 141.7 (s, C_{ipso}, Ph), 137.6 (s, $SnPh_2Cl$), 133.2 (s, Ph), 131.4 (s, Ph), 127.5 (s, $SnPh_2Cl$), 127.3 (s, $SnPh_2Cl$), 120.2 (s, Ph), 27.9 (vt, N = 25.3, PCH(CH_3)$_2$), 23.1 (s, CH$_3$CO), 20.1, 19.3 (both s, PCH(CH_3)$_2$). $^{119}Sn\{^1H\}$ NMR (111.83 MHz, C_6D_6, 293K): δ 15.2 (t, $J_{P-^{119}Sn}$ = 113). $T_{1(min)}$ (ms, OsH_2, 300 MHz, C_7D_8, 238 K): 81 ± 4 (−11.03, −13.0 ppm).

Preparation of $OsH_2(SnPh_2Cl)\{C_6H_4C(O)C_6H_5\}(P^iPr_3)_2$ (3). Benzophenone (40.2 mg, 0.22 mmol) was added to a solution of **1** (116 mg, 0.147 mmol) in toluene (10 mL). After stirring for 5 days at room temperature the color of the solution had changed to orange-red. The resulting solution was filtered through Celite and was taken to dryness. Subsequent addition of pentane caused the precipitation of a dark red solid, which was washed with pentane and dried in vacuo. Yield: 92 mg (62%). Anal. Calcd for $C_{43}H_{63}ClOOsP_2Sn$: C, 51.53; H, 6.34. Found: C, 51.75; H, 5.99. IR (Nujol, cm^{-1}): ν(OsH) 2114 (w), ν(CO) 1666 (m). ^1H NMR (300 MHz, C_7D_8, 303 K): δ 8.35 (d, J_{H-H} = 6.9, 4H, SnPh−H_{ortho}), 7.92 (d, J_{H-H} = 7.5, 2H, Ph), 7.81 (d, J_{H-H} = 6.9, 1H, Os−C_6H_4), 7.25−7.02 (m, 10H, $SnPh_2$-Cl, Os−C_6H_4 and Ph), 6.88 (t, J_{H-H} = 6.9, 1H, Os−C_6H_4), 6.75 (t, J_{H-H} = 6.9, 1H, Os−C_6H_4), 2.22 (m, 6H, PCH(CH_3)$_2$), 1.00 (dvt, N = 13.5, J_{H-H} = 6.9, 18H, PCH(CH_3)$_2$), 0.73 (dvt, N = 13.5, J_{H-H} = 6.9, 18H, PCH(CH_3)$_2$), −11.40 (br, 2H, OsH). ^1H NMR (300 MHz, C_7D_8, 233 K, hydride region): δ −10.45 (part A of an ABX_2 spin system, 1H, J_{A-X} = 9, J_{A-B} = 42), −12.54 (part B of an ABX_2 spin system, 1H, J_{B-X} = 12.6, J_{A-B} = 42). $^{31}P\{^1H\}$ NMR (121.42 MHz, C_7D_8, 293 K): δ 7.9 (s with tin satellites $J_{P-^{119}Sn} = J_{P-^{117}Sn}$ = 119). $^{31}P\{^1H\}$ NMR (121.42 MHz, C_7D_8, 193 K): δ 7.7 (AB spin system, $\Delta\nu$ = 578 Hz, J_{A-B} = 195). $^{13}C\{^1H\}$ NMR (75.42 MHz, C_6D_6, 293 K): δ 208.5 (s, CO), 198.1 (t, J_{P-C} = 7, OsC), 156.3 (s, $SnPh_2Cl$−C_{ipso}), 144.1 (s, Ph), 140.5 (s, Ph), 137.6 (s, $SnPh_2Cl$), 137.4, 134.2, 132.8, 132.2, 132.0, 131.8, 130.1, 128.7 (all s, Ph), 127.4 (s, $SnPh_2Cl$), 127.2 (s, $SnPh_2Cl$), 120.4 (s, Ph), 28.2 (vt, N = 25, PCH(CH_3)$_2$), 20.4, 19.6 (both s, PCH(CH_3)$_2$). $^{119}Sn\{^1H\}$ NMR (111.83 MHz, C_6D_6, 293 K): δ 18.2 (t, $J_{P-^{119}Sn}$ = 119). $T_{1(min)}$ (ms, OsH_2, 300 MHz, C_7D_8, 243 K): 81 ± 4 (−10.40, −12.53 ppm).

Preparation of $OsHD(SnPh_2Cl)\{C_6D_4C(O)C_6D_5\}(P^iPr_3)_2$ (3-d_{10}). Benzophenone-d_{10} (37.2 mg, 0.23 mmol) was added to a solution of **1** (107 mg, 0.135 mmol) in toluene (10 mL). After stirring for 5 days at room temperature the color of the solution had changed to orange-red. The resulting solution was filtered through Celite and was taken to dryness. Subsequent addition of pentane caused the precipitation of a dark red solid, which was washed with pentane and dried in vacuo. Yield: 70 mg (52%). ^1H NMR (300 MHz, C_7D_8, 293 K): δ 8.35 (d, J_{H-H} = 7.2, 4H, SnPh−H_{ortho}), 7.25 (t, J_{H-H} = 7.2, 4H, SnPh−H_{meta}), 7.15 (t, J_{H-H} = 7.2, 2H, SnPh−H_{para}), 2.22 (m, 6H, PCH(CH_3)$_2$), 1.00 (dvt, N = 13.5, J_{H-H} = 6.9, 18H, PCH(CH_3)$_2$), 0.76 (dvt, N = 13.5, J_{H-H} = 6.9, 18H, PCH(CH_3)$_2$), −11.20 (br, 1H, OsH). ^1H NMR (300 MHz, C_7D_8, 233 K, hydride region): δ −10.45 (t, J_{H-P} = 9, 0.5H), −12.60 (t, J_{H-P} = 12.6, 0.5H). $^{31}P\{^1H\}$ NMR (121.42 MHz, C_7D_8, 293 K): δ 8.0 (s with tin satellites J_{P-Sn} = 112). ^2H NMR (46.1 MHz, C_7H_8, 263 K): δ 9.0−6.0 (m, 9D, C_6D_5, C_6D_4), −10.4 (br, 0.5D, OsD), −12.5 (br, 0.5D, OsD).

Preparation of $OsH_2(SnPh_2Cl)\{C_6H_4C(O)C_6F_5\}(P^iPr_3)_2$ (4). 2,3,4,5,6-Pentafluorobenzophenone (77.6 mg, 0.28 mmol) was added to a solution of **1** (150 mg, 0.19 mmol) in toluene (10 mL). After stirring for 1 week at room temperature, the resulting solution was filtered through Celite and was taken to dryness. Subsequent addition of pentane caused the precipitation of a dark red solid, which was washed with pentane and dried in vacuo. Yield: 129.8 mg (65%). Anal. Calcd for $C_{43}H_{58}Cl\,F_5OOsP_2Sn$: C, 47.29; H, 5.35. Found: C, 47.23; H, 5.13. IR (Nujol, cm^{-1}): ν(OsH) 2236 (w), ν(CO) 1652 (m), ν(C−F) 1522 (s). ^1H NMR (300 MHz, C_7D_8, 293 K): δ 8.22 (d, J_{H-H} = 6.9, 4H, SnPh−H_{ortho}), 8.22 (d, J_{H-H} = 6.9, 1H, Os−C_6H_4), 7.31 (d, J_{H-H} = 6.9, 1H, Os−C_6H_4), 7.14 (t, J_{H-H} = 6.9, 4H, SnPh−H_{meta}), 7.01 (t, J_{H-H} = 6.9, 2H, SnPh−H_{para}), 6.69 (t, J_{H-H} = 6.9, 2H, Os−C_6H_4), 2.14 (m, 6H, PCH(CH_3)$_2$), 0.87

(dvt, N = 13.5, J_{H-H} = 6.9, 18H, PCH(CH_3)$_2$), 0.65 (dvt, N = 13.5, J_{H-H} = 6.9, 18H, PCH(CH_3)$_2$), −10.28 (br, 1H, OsH), −12.38 (br, 1H, OsH). ^{1}H NMR (300 MHz, C_7D_8, 233 K, hydride region): δ −10.12 (part A of an ABX_2 spin system, 1H, J_{A-X} = 11.7, J_{A-B} = 25), −12.50 (part B of an ABX_2 spin system, 1H, J_{B-X} = 15, J_{A-B} = 25). ^{31}P{^{1}H} NMR (121.42 MHz, C_7D_8, 293 K): δ 8.4 (s with tin satellites $J_{P-^{119}Sn}$ = $J_{P-^{117}Sn}$ = 114). ^{31}P{^{1}H} NMR (121.42 MHz, C_7D_8, 183 K): δ 6.8 (AB spin system, $\Delta\nu$ = 863 Hz, J_{A-B} = 197). ^{13}C{^{1}H} NMR (75.42 MHz, C_6D_6, 293 K): δ 203.4 (t, J_{C-F} = 6.9, *C*O), 194.0 (m, Os*C*), 155.6 (s, $SnPh_2Cl$), 144.8 (d, J_{C-F} = 258.2, C_6F_5), 144.1 (s, OsPh), 141.1 (s, OsPh), 138.4 (d, J_{C-F} = 272, C_6F_5), 137.1 (s, $SnPh_2Cl$), 133.1 (s, OsPh), 133 (s, OsPh), 127.5 (s, $SnPh_2Cl$), 127.4 (s, $SnPh_2$-Cl), 120.6 (s, OsPh), 28.6 (vt, N = 25.6, P*C*H(CH$_3$)$_2$), 20.2, 19.3 (both s, PCH(*C*H$_3$)$_2$). ^{19}F NMR (282.33 MHz, C_6D_6, 293 K): δ −136.6 (m, 2F, *o*-F), −149.5 (t, 1F, J_{F-F} = 22, *p*-F), −160.9 (m, 2F, *m*-F). ^{119}Sn{^{1}H} NMR (111.83 MHz, C_6D_6, 293 K): δ 7.9 (t, $J_{P-^{119}Sn}$ = 114). $T_{1(min)}$ (ms, OsH_2, 300 MHz, C_7D_8, 248 K): 85 ± 2 (−10.07, −12.55 ppm).

Preparation of $OsH_2(SnPh_2Cl)\{C_6H_3FC(O)CH_3\}(P^iPr_3)_2$ (5). 2-Fluoroacetophenone (25 μL, 0.202 mmol) was added to a solution of **1** (106 mg, 0.135 mmol) in toluene (10 mL). After stirring for 3 days at room temperature the color of the solution had changed to orange. The resulting solution was filtered through Celite and was taken to dryness. Subsequent addition of pentane caused the precipitation of an orange solid, which was washed with pentane and dried in vacuo. Yield: 82 mg (63%). Anal. Calcd for $C_{38}H_{60}ClFOOsP_2Sn$: C, 47.63; H, 6.31. Found: C, 47.92; H, 6.31. IR (Nujol, cm^{-1}): ν(OsH) 2086 (w), ν(CO) 1603 (s). ^{1}H NMR (300 MHz, C_7D_8, 303 K): δ 8.34 (d, J_{H-H} = 7.5, 4H, SnPh−H_{ortho}), 7.91 (d, J_{H-H} = 7.8, 1H, Os−C_6H_3F), 7.31 (t, J_{H-H} = 7.5, 4H, SnPh−H_{meta}), 7.17 (t, J_{H-H} = 7.5, 2H, SnPh−H_{para}), 6.63 (vtd, J_{H-H} = 7.8, J_{H-F} = 13, 1H, Os−C_6H_3F), 6.35 (dd, J_{H-H} = 7.8, J_{H-F} = 12, 1H, Os−C_6H_3F), 2.90 (d, J_{H-F} = 5, 3H, CH_3), 2.15 (m, 6H, PC*H*(CH$_3$)$_2$), 0.95 (dvt, J_{H-H} = 6.6, N = 12.9, 18H, PCH(CH_3)$_2$), 0.70 (dvt, J_{H-H} = 6.6, N = 12.9, 18H, PCH(CH_3)$_2$), −11.66 (br, 2H, OsH). ^{1}H NMR (300 MHz, C_7D_8, 233 K, hydride region): δ −10.65 (part A of an ABX_2 spin system, 1H, J_{A-X} = 8.3, J_{A-B} = 59), −12.70 (part B of an ABX_2 spin system, 1H, J_{B-X} = 12.5, J_{A-B} = 59). ^{31}P{^{1}H} NMR (121.42 MHz, C_7D_8, 293 K): δ 7.1 (s with tin satellites $J_{P-^{119}Sn}$ = $J_{P-^{117}Sn}$ = 115). ^{31}P{^{1}H} NMR (121.42 MHz, C_7D_8, 183 K): δ 6.1 (AB spin system, $\Delta\nu$ = 705 Hz, J_{A-B} = 203). ^{13}C{^{1}H} NMR (75.42 MHz, C_6D_6, 293 K): δ 210.6 (dt, J_{C-F} = 5.5, J_{C-P} = 2, *C*O), 198.7 (dt, J_{C-F} = J_{C-P} = 5.5, Os*C*), 166.0 (d, J_{C-F} = 263.2, Ph), 155.9 (s, C_{ipso}, $SnPh_2Cl$), 139.4 (d, J_{C-F} = 3.2, Ph), 137.5 (s, $SnPh_2Cl$), 134.4 (d, J_{C-F} = 8.3, Ph), 130.5 (d, J_{C-F} = 6.4, Ph), 127.5 (s, $SnPh_2Cl$), 127.3 (s, $SnPh_2$-Cl), 106.1 (d, J_{C-F} = 21.6, Ph), 28.3 (t, J_{C-F} = 9.6, *C*H$_3$), 27.9 (vt, N = 24.8, P*C*H(CH$_3$)$_2$), 20.1, 19.3 (both s, PCH(*C*H$_3$)$_2$). ^{19}F NMR (282.33 MHz, C_6D_6, 293 K): δ −109. 8 (m). ^{119}Sn{^{1}H} NMR (111.83 MHz, C_6D_6, 293 K): δ 12.3 (dt, $J_{P-^{119}Sn}$ = 115, $J_{F-^{119}Sn}$ = 41). $T_{1(min)}$ (ms, OsH_2, 300 MHz, C_7D_8, 248 K): 79 ± 4 (−10.65, −12.70 ppm).

Preparation of $OsH_2(SnPh_2Cl)\{C_6H_4C(NH)C_6H_5\}(P^iPr_3)_2$ (6). Benzophenone imine (34.7 mg, 0.191 mmol) was added to a solution of **1** (100 mg, 0.127 mmol) in toluene (10 mL). After stirring for 40 h at room temperature the color of the solution had changed from pale yellow to orange. The resulting solution was taken to dryness. Subsequent addition of pentane caused the precipitation of an orange solid, which was washed with pentane and dried in vacuo. Yield: 122 mg (97%). Anal. Calcd for $C_{43}H_{64}ClNOsP_2Sn$: C, 50.99; H, 6.52; N, 1.39. Found: C, 51.20; H, 6.33; N, 1.23. IR (Nujol, cm^{-1}): ν(N−H) 3246 (m), ν(Os−H) 2077 (w), ν(C═N) 1579 (s). ^{1}H NMR (300 MHz, C_7D_8, 293 K): δ 12.83 (s with tin satellites $J_{H-^{117}Sn}$ = $J_{H-^{119}Sn}$ = 77, 1H, C═N*H*), 8.39 (d, J_{H-H} = 7.5, 1H, Os−C_6H_4), 8.13 (d, J_{H-H} = 7.2, 4H, SnPh−H_{ortho}), 7.84 (d, J_{H-H} = 7.5, 2H$_{ortho}$, Ph), 7.66 (d, J_{H-H} = 7.5, 1H, Os−C_6H_4), 7.25 (t, J_{H-H} = 7.5, 2H$_{meta}$, Ph), 7.17 (t, J_{H-H} = 7.2, 4H, SnPh−H_{meta}), 7.10 (t, J_{H-H} = 7.5, 1H$_{para}$, Ph), 6.99 (t, J_{H-H} = 7.2, 2H, SnPh−H_{para}), 6.95 (t, J_{H-H} = 7.5, 1H, Os−C_6H_4), 6.92 (t, J_{H-H} = 7.5, 1H, Os−C_6H_4), 1.98 (m, 6H, PC*H*(CH$_3$)$_2$), 1.05 (dvt, J_{H-H} = 6.6, N = 13.2, 18H, PCH(CH_3)$_2$), 0.71 (dvt, J_{H-H} = 6.6, N = 13.2, 18H, PCH(CH_3)$_2$), −9.79 (t, J_{P-H} = 14.4, 2H, OsH). ^{31}P{^{1}H} NMR (121.42 MHz, C_7D_8, 293 K): δ 2.7 (s with tin satellites $J_{P-^{119}Sn}$ = $J_{P-^{117}Sn}$ = 107). ^{31}P{^{1}H} NMR (121.42 MHz, C_7D_8, 183 K): δ 3.7 (AB spin system, $\Delta\nu$ = 879 Hz, J_{A-B} = 202), −0.8 (s). ^{13}C{^{1}H} NMR (75.47 MHz, C_6D_6, 293 K): δ 181.3 (t, J_{C-P} = 2, *C*═N), 178.1 (t, J_{C-P} = 8, Os*C*), 156.2 (s, C_{ipso}, $SnPh_2Cl$), 145.0 (s, C_{ipso}, Ph), 144.6 (s, Ph), 137.7 (s, C_{ipso}, Ph), 135.1 (s, $SnPh_2Cl$), 130.2 (s, Ph), 130.1 (s, Ph), 129.9 (s, Ph), 129.2 (s, $SnPh_2Cl$), 128.7 (s, Ph), 127,6 (s, $SnPh_2Cl$), 127.2 (s, Ph), 120.4 (s, Ph), 27.8 (vt, N = 24.8, P*C*H(CH$_3$)$_2$), 20.2, 19.4 (both s, PCH(*C*H$_3$)$_2$). ^{119}Sn{^{1}H} NMR (111.83 MHz, C_6D_6, 293 K): δ 0.3 (t, $J_{P-^{119}Sn}$ = 107). $T_{1(min)}$ (ms, OsH_2, 300 MHz, C_7D_8, 243 K): 81 ± 1 (−9.87 ppm).

Preparation of $OsH_2(SnPh_2OH)\{C_6H_4C(NH)C_6H_5\}(P^iPr_3)_2$ (7). KOH (7.8 mg, 0.14 mmol) was added to a solution of **6** (121 mg, 0.122 mmol) in THF (10 mL). After stirring for 2 days at room temperature, the resulting suspension was filtered through Celite and the solution was taken to dryness. Subsequent addition of pentane caused the precipitation of an orange solid, which was washed with pentane and dried in vacuo. Yield: 89 mg (78%). Anal. Calcd for $C_{43}H_{65}NOOsP_2Sn\cdot C_5H_{12}$: C, 54.49; H, 7.28; N, 1.32. Found: C, 54.10; H, 6.91; N, 1.92. IR (Nujol, cm^{-1}): ν(SnOH) 3594 (w), ν(NH) 3167, ν-(OsH) 2159 (w), ν(SnOH) 1670 (w), ν(C═N) 1577 (m). ^{1}H NMR (300 MHz, C_7D_8, 293 K): δ 14.07 (s with tin satellites $J_{H-^{119}Sn}$ = $J_{H-^{117}Sn}$ = 75, 1H, C═N*H*), 8.41 (d, J_{H-H} = 7.5, 1H, Os−C_6H_4), 7.86 (d, J_{H-H} = 7.5, 4H, SnPh−H_{ortho}), 7.76 (d, J_{H-H} = 7.5, 1H, Ph), 7.63 (d, J_{H-H} = 7.5, 1H, Os−C_6H_4), 7.29 (t, J_{H-H} = 7.5, 2H, Ph), 7.18 (t, J_{H-H} = 7.5, 4H, SnPh−H_{meta}), 7.10−6.97 (m, 5H, Ph, Os−C_6H_4, SnPh−H_{para}), 6.90 (t, J_{H-H} = 7.5, 1H, Os−C_6H_4), 2.12 (m, 6H, PC*H*(CH$_3$)$_2$), 1.10 (dvt, N = 12.9, J_{H-H} = 6.6, 18H, PCH(CH_3)$_2$), 0.75 (dvt, N = 12.9, J_{H-H} = 6.6, 18H, PCH(CH_3)$_2$), 0.65 (s with tin satellites $J_{H-^{119}Sn}$ = $J_{H-^{117}Sn}$ = 34, 1H, $SnPh_2OH$), −9.90 (br, 2H, OsH). ^{31}P{^{1}H} NMR (121.42 MHz, C_7D_8, 293 K): δ 5.1 (s with tin satellites $J_{P-^{119}Sn}$ = $J_{P-^{117}Sn}$ = 108). ^{31}P{^{1}H} NMR (121.42 MHz, C_7D_8, 183 K): δ 2.9 (AB spin system, $\Delta\nu$ = 1094 Hz, J_{A-B} = 237), −0.1 (s). ^{13}C-{^{1}H} NMR (75.42 MHz, C_6D_6, 293 K): δ 180.2 (t, J_{C-P} = 2, *C*═N), 180.0 (t, J_{C-P} = 8, Os*C*), 157.0 (s, $SnPh_2OH$), 145.7, 144.7, 138.5, 137.2 (all s, Ph), 135.0 (s, $SnPh_2OH$), 130.1, 129.9, 129.8, 129.6 (all s, Ph), 129.4 (s, $SnPh_2OH$), 129.2 (s, Ph), 127.6 (s, $SnPh_2OH$), 127.0 (s, Ph), 119.9 (s, Ph), 27.7 (vt, N = 25.3, P*C*H(CH$_3$)$_2$), 19.8, 19.1 (both s, PCH(*C*H$_3$)$_2$). ^{119}Sn{^{1}H} NMR (111.83 MHz, C_6D_6, 293 K): δ −98.1 (t, $J_{P-^{119}Sn}$ = 108). $T_{1(min)}$ (ms, 300 MHz, OsH_2, C_7D_8, 243 K): 84 ± 6 (−9.98 ppm).

Structural Analysis of Complexes 2, 6, and 7. X-ray data were collected for all complexes at low temperature on a Bruker Smart APEX CCD diffractometer at 173.0(2) (**2** and **6**) or 100.0(2) (**7**) K equipped with a normal focus, 2.4 kW sealed tube source (molybdenum radiation, λ = 0.71073 Å) operating at 50 kV and 40 mA (**2** and **7**) or 40 kV and 20 mA (**6**). Data were collected over a hemisphere by a combination of three sets (**2** and **6**) or over the complete sphere by a combination of four sets (**7**). Each frame exposure time was 30 s (**2**) or 10 s (**6** and **7**) covering 0.3° in ω. Data were corrected for absorption by using a multiscan method applied with the SADABS[40] program. The structures for all five compounds were solved by the Patterson method. Refinement, by full-matrix least squares on F^2 with SHELXL97,[41] was similar for all complexes, including isotropic and subsequently anisotropic displacement parameters for all non-hydrogen atoms. The hydrogen atoms were observed or calculated and refined freely

(40) Blessing, R. H. *Acta Crystallogr.* **1995**, *A51*, 33−38. *SADABS*, Area-detector absorption correction; Bruker-AXS: Madison, WI, 1996.
(41) *SHELXTL* Package v. 6.10; Bruker-AXS: Madison, WI, 2000. Sheldrick, G. M. *SHELXS-86* and *SHELXL-97*; University of Göttingen: Göttingen, Germany, 1997.

Table 8. Crystal Data and Data Collection and Refinement for 2, 6, and 7

	2	6	7
		Crystal Data	
formula	$C_{38}H_{61}ClOOsP_2Sn$	$C_{43}H_{64}ClNOsP_2Sn$	$C_{43}H_{65}NOOsP_2Sn\cdot0.5C_5H_{12}$
molecular wt	940.15	1001.23	1018.86
color and habit	orange, irregular block	orange, prism	orange, prism
symmetry, space group	orthorhombic, *Pnma*	monoclinic, $P2_1/n$	monoclinic, $C2/c$
a, Å	15.5246(11)	10.0417(9)	21.4026(8)
b, Å	21.2225(15)	21.5041(19)	17.8230(8)
c, Å	11.8693(8)	19.8536(17)	23.8124(11)
β, deg		98.572(2)	106.176(1)
V, Å^3	3910.6(5)	4239.3(6)	8723.8(6)
Z	4	4	8
D_{calc}, g cm^{-3}	1.597	1.569	1.551
		Data Collection and Refinement	
diffractometer		Bruker Smart APEX	
λ(Mo Kα), Å		0.71073	
monochromator		graphite oriented	
scan type		ω scans	
μ, mm^{-1}	4.062	3.752	3.590
2θ, range deg	3, 57	3, 57	3, 57
temp, K	173	173	100
no. of data collected	25 020	27 818	52 613
no. of unique data	4894 (R_{int}=0.0570)	10 029 (R_{int}=0.0469)	10 526 (R_{int}=0.0707)
no. of params/restraints	229/0	464/0	491/3
R_1[a] [$F^2 > 2\sigma(F^2)$]	0.0278	0.0363	0.0318
wR_2[b] [all data]	0.0484	0.0810	0.0953
S[c] [all data]	0.750	1.030	0.971

[a] $R_1(F) = \sum||F_o| - |F_c||/\sum|F_o|$. [b] $wR_2(F^2) = \{\sum[w(F_o^2 - F_c^2)^2]/\sum[w(F_o^2)^2]\}^{1/2}$. [c] Goof $= S = \{\sum[F_o^2 - F_c^2)^2]/(n - p)\}^{1/2}$, where n is the number of reflections and p is the number of refined parameters.

or using a restricted riding model. Hydride ligands were observed in the difference Fourier maps and refined as free isotropic atoms with the same (**2**) or individual thermal parameters (**6** and **7**). A region of disordered solvent was observed in **7** close to an axis of symmetry and was refined as isotropic pentane with geometrical restraints. All the highest electronic residuals were observed in close proximity to the Os centers and make no chemical sense. Crystal data and details of the data collection and refinement are given in Table 8.

Computational Details

DFT optimizations were carried out with the Gaussian98[42] series of programs using the B3LYP functional.[43] Calculations were carried out on model complexes. For the mechanistic studies, single-point calculations at the CCSD(T) level of theory were carried out on the B3LYP geometries using the same basis set. Modelization of the phosphine ligands was done as follows: one P^iPr_3 was modeled as PH_3, whereas the $P\{C(CH_3)=CH_2\}^iPr_2$ group was modeled as $P\{C(CH_3)=CH_2\}H_2$. The $SnPh_2X$ (X = Cl, OH) ligand was modeled by $Sn(CH=CH_2)_2X$.

A quasi-relativistic effective core potential operator was used to represent the innermost electrons of the osmium and tin atoms.[44] The basis set for the osmium and tin atoms was that associated with the pseudopotential with a standard valence double-ζ LANL2DZ contraction.[42] A 6-31G(d) basis set was used for the phosphorus and nitrogen.[45] Hydrogens directly attached to the metal were described using a 6-31G(p) basis set, while a 6-31G basis set was used for the rest of the hydrogens.[45] A 6-31G basis set[45] was also used for the chlorine and all the carbon atoms.

Acknowledgment. We acknowledge financial support from the Spanish MCYT (Project No. BQU2002-00606 and BQU2002-04110-C02-02). The use of computational facilities of the Centre de Supercomputació de Catalunya (C^4) is gratefully appreciated. M.O. and G.U. acknowledge the Spanish MCYT for funding through the "Ramón y Cajal" Program.

Supporting Information Available: Tables of positional and displacement parameters, crystallographic data, and bond lengths and angles. This material is available free of charge via the Internet at http://pubs.acs.org.

OM030229Y

(42) Frisch, M. J.; Trucks, G. W.; Schlegel, H. B.; Scuseria, G. E.; Robb, M. A.; Cheeseman, J. R.; Zakrzewski, V. G.; Montgomery, J. A., Jr.; Stratmann, R. E.; Burant, J. C.; Dapprich, S.; Millam, J. M.; Daniels, A. D.; Kudin, K. N.; Strain, M. C.; Farkas, O.; Tomasi, J.; Barone, V.; Cossi, M.; Cammi, R.; Mennucci, B.; Pomelli, C.; Adamo, C.; Clifford, S.; Ochterski, J.; Petersson, G. A.; Ayala, P. Y.; Cui, Q.; Morokuma, K.; Malick, D. K.; Rabuck, A. D.; Raghavachari, K.; Foresman, J. B.; Cioslowski, J.; Ortiz, J. V.; Stefanov, B. B.; Liu, G.; Liashenko, A.; Piskorz, P.; Komaromi, I.; Gomperts, R.; Martin, R. L.; Fox, D. J.; Keith, T.; Al-Laham, M. A.; Peng, C. Y.; Nanayakkara, A.; Gonzalez, C.; Challacombe, M.; Gill, P. M. W.; Johnson, B.; Chen, W.; Wong, M. W.; Andres, J. L.; Gonzalez, C.; Head-Gordon, M.; Replogle, E. S.; Pople, J. A. *Gaussian 98*, Revision A.6; Gaussian Inc.: Pittsburgh, PA, 1998.

(43) (a) Lee, C.; Yang, W.; Parr, R. G. *Phys. Rev. B* **1988**, *37*, 785. (b) Becke, A. D. *J. Chem. Phys.* **1993**, *98*, 5648. (c) Stevens, P. J.; Devlin, F. J.; Chabalowski, C. F.; Frisch, M. J. *J. Phys. Chem.* **1994**, *98*, 11623.

(44) Hay, P. J.; Wadt, W. R. *J. Chem. Phys.* **1985**, *82*, 299.

(45) (a) Hehre, W. J.; Ditchfield, R.; Pople, J. A. *J. Chem. Phys.* **1972**, *56*, 2257. (b) Hariharan, P. C.; Pople, J. A. *Theor. Chim. Acta* **1973**, *28*, 213. (c) Francl, M. M.; Pietro, W. J.; Hehre, W. J.; Binkley, J. S.; Gordon, M. S.; DeFrees, D. J.; Pople, J. A. *J. Chem. Phys.* **1982**, *77*, 3654.